

Superradiant emission spectra of a two-qubit system in circuit quantum electrodynamics

Ya. S. Greenberg* and O. A. Chuikin

Novosibirsk State Technical University, Novosibirsk, Russia

(Dated: June 30, 2022)

In this paper we study the spontaneous emission spectra and the emission decay rates of a simplest atom system that exhibits sub- and superradiant properties: a system which consists of two artificial atoms (superconducting qubits) embedded in a one-dimensional open waveguide. The calculations are based on the method of the transition operator which was firstly introduced by R. H. Lehmberg to theoretically describe the spontaneous emission of two-level atoms in a free space. We obtain the explicit expressions for the photon radiation spectra and the emission decay rates for different initial two-qubit configurations with one and two excitations. For every initial state we calculate the radiation spectra and the emission decay rates for different effective distances between qubits. In every case, a decay rate is compared with a single qubit decay to show the superradiant or subradiant nature of a two-qubit decay with a given initial state.

I. INTRODUCTION

The control of spontaneous emission in the multi-atom (or qubit) system that interact with a quantized radiation field in restricted geometries has received a great deal of attention in recent years (see review paper [1] and references therein). This can be achieved in various physical set-ups, for example, by putting two-level atoms in an optical cavity [2], by embedding them in a nanophotonic waveguide [3] or by coupling superconducting qubits to a transmission line resonator [4–6]. Due to spatial confinements, these set-ups allow one to achieve an almost ideal mode matching which results in a strong coupling [7] and even ultrastrong coupling regimes when the interaction strength overwhelms relaxation rates [8]. These experimental conditions are very challenging to obtain for regular atoms in optical domain.

The interaction of excited atoms with the continuum of the environment modes leads to spontaneous emission which is one of the major sources of decoherence. The spontaneous emission results in irreversible loss of the information encoded in the internal states of the system and thus is regarded as the main obstacle in practical implementations of quantum processing.

The early studies of spontaneous emission in multi- and two-atom systems deal mainly with atoms placed in a free space environment [9–14]. In this case, the interaction of atoms with the vacuum modes gives rise to short range dipole-dipole interaction between the atoms [9]. The spontaneous emission of excited atom in free space is the result of interaction of the atom with the continuum modes of the vacuum. A collection of N identical two level excited atoms undergoes a spontaneous coherent transition to the ground state, which is accompanied by the emission of N photons, the intensity of which scales as N^2 , and the decay rate of which is NT , where

Γ is the decay rate of an isolated atom [15]. Therefore, the N excited atoms decay N times faster than an isolated atom. This property of N atom system was named superradiance [16, 17].

However, the behaviour of atoms in a confined geometry is quite different from that in a free space. For example, a spontaneous decay rate of an atom embedded in a resonator may significantly differ from its decay rate in a free space (so called Purcell effect) [18]. The exchange of the virtual photons between the identical equally spaced atoms in a one-dimensional waveguide results in an infinite-range inter-atomic interaction the strength of which periodically depends on the ratio d/λ , where d is the distance between neighbour atoms, λ is the wavelength of the guiding mode. Furthermore, this system exhibits collective excitations with lifetimes from extremely sub- to superradiant values relative to the radiative lifetime of the individual atom [19–23].

Many of these effects have experimentally been realized within the frame of circuit quantum electrodynamics (QED) with superconducting qubits as artificial atoms [4]. A significant difference between natural atoms and superconducting qubits is that in circuit QED we can create artificial atoms with desirable parameters some of which can be tuned, e.g. resonant frequency or coupling strength [24]. What is more important, we can address and manipulate the artificial atoms individually [25]. This makes it possible to in-depth study of different types of interaction between a few qubits which can be far more interesting and complex than just one qubit in a cavity [11, 26]. Because of the perfect mode matching the exchange interaction between the qubits is very strong and critically depends on the effective distance between them which can be tuned by changing the wavelength via qubit resonant frequency. Different spatial arrangements of qubits in a chain can lead to significant modification of decay rates [27, 28]. This collective effect may lead to both the enhancement of a decay rate, which is called superradiance [29, 30], and the reduction of the decay rate, which corresponds to subradiance [19, 20].

The arrangement consisting of two interacting atoms is

*Electronic address: yakovgreenberg@yahoo.com

a simplest system which exhibits sub- and superradiant properties. This system has been extensively studied in the frame of 1D circuit quantum electrodynamics [21, 23, 26–29, 31, 32].

In this paper we consider a system which consists of two artificial atoms (superconducting qubits) in a one-dimensional open waveguide. In contrast to previous studies, we obtain here the general explicit expression which allows us to calculate the radiation photon spectra and the emission decay rates (decay rates of the energy loss) for different initial two-qubit configurations with one and two excitations and for different values of the ratio d/λ . We systematically compare two-qubit spontaneous emission spectra with those of a single qubit. We show that depending on the ratio d/λ , there exist both superradiant states when a decay rate of initial two-qubit configuration exceeds that of a single qubit and subradiant states when a decay rate of initial two-qubit configuration is less than that of a single qubit. Our results for $d/\lambda \ll 1$ are consistent with those which has experimentally been observed for two superconducting qubits in a low quality cavity [33].

There exist two approaches which allow us to perform these calculations. The most common method uses the master equation for the reduced density matrix in the Lindblad form [27]. The second approach uses the Heisenberg equation of motion for arbitrary system operator [9, 10]. Two approaches are, of course, equivalent. The choice in favour of either of these methods depends on the problem at hand.

Here we choose the second method and take as a system operator the so-called transition operator, firstly introduced by Lehmann [34] to theoretically describe the spontaneous emission of two-level atoms in free space [9, 10]. The exact expressions for the matrix elements of the transition operator can be obtained within standard quantum mechanics formalism using Heisenberg equations. The tracing out the photonic modes from the equations of motion allows us to obtain equations only for atomic operators independent of the photon number. As distinct from conventional density matrix approach, differential equations for the matrix elements of the transition operator are linear in a basis set of a spin system and, therefore, it is easier to solve them analytically. Moreover, because the solutions of equations are operator functions, they are independent of the specific initial state of the system. It means that we don't need to find a new solution for every new initial state like in the case of equations for the density matrix. Once the exact solutions for transition operators are found, we can use them not only to obtain transition probabilities but also for the calculation of the photonic emission spectrum for arbitrary initial density matrix. As we show here, transition operators and elements of the density matrix are very closely related, so one can easily switch from one approach to the other one if needed.

The paper is organized as follows. In Sec. 2 we define the transition operator, describe its general proper-

ties, and establish its connection to a density matrix. In Sec. 3 we show the application of the method for the description of N -qubit system in a 1D transmission line and obtain general equation of motion for the matrix elements of transition operators. In Sec. 4 we present a general expression for the spectral density of photons in terms of two-time correlation functions of spin operators and show how these types of correlation functions can be calculated in terms of the vacuum average of transition operators and initial density matrix. In Sec. 5 we apply our method to a two-qubit system and find the diagonal and off-diagonal matrix elements of the transition operator. In Sec. 6 we calculate the probabilities of different transitions between the states in a two-qubit system, which contribute to the radiation spectra and the photon emission decay rates. The main results of our paper are presented in Sec. 7. In this section we obtain the general expressions which allow us to calculate both the radiation spectra and the emission decay rates for arbitrary initial states of a two-qubit system. For every initial state we consider in Sec. 7, we calculate the radiation spectra and the emission decay rates for different effective distances between qubits. In every case, a decay rate is compared with a single qubit decay to show the superradiant or subradiant nature of a two-qubit decay with a given initial state. A summary of our work is presented in concluding Sec. 8.

II. GENERAL PROPERTIES OF TRANSITION OPERATOR

We consider a system of N identical qubits with eigenstates $|i\rangle$ coupled to a continuum of photon modes $|\nu\rangle$ in a one-dimensional open waveguide. Our main interest is the probability of transition from some arbitrary initial state of a qubit system $|\Psi_0\rangle$ with no photons to some final state $|\Psi_1\rangle$ with ν photons in the field. According to the general principles of quantum mechanics, the probability amplitude of such transition is given by the following matrix element:

$$\langle\Psi_1, \nu|e^{-iHt}|\Psi_0, 0\rangle, \quad (1)$$

where H is the complete Hamiltonian which includes the N -qubit system, photon field, and their interaction, $|0\rangle$, $|\nu\rangle$ are the Fock states with zero and ν photons, respectively. To find the total transition probability we must find the squared modulus of this amplitude and sum it over the complete set of possible final photon states $|\mu\rangle$ for the field.

$$W_{0\rightarrow 1} = \sum_{\mu} |\langle\Psi_1, \mu|e^{-iHt}|\Psi_0, 0\rangle|^2 \quad (2)$$

Using the completeness of the set of the photon states $\sum_{\mu} |\mu\rangle\langle\mu| = 1$, we rewrite (2) as follows:

$$W_{0 \rightarrow 1} = \langle \Psi_0 | \langle 0 | e^{iHt} | \Psi_1 \rangle \langle \Psi_1 | e^{-iHt} | 0 \rangle | \Psi_0 \rangle \quad (3)$$

By expanding wave function $|\Psi_1\rangle$ over the complete set of qubit states $|i\rangle$ with some coefficients c_i we can rewrite (3) in the following form:

$$W_{0 \rightarrow 1} = \sum_{i,j} c_i c_j^* \langle \Psi_0 | \langle e^{iHt} | i \rangle \langle j | e^{-iHt} \rangle_0 | \Psi_0 \rangle, \quad (4)$$

where $\langle \dots \rangle_0$ is the average over photon vacuum $\langle \dots \rangle_0 = \langle 0 | \dots | 0 \rangle$

Following Lehmborg [34], we define a transition operator:

$$P_{i,j}(t) = e^{iHt} |i\rangle \langle j| e^{-iHt}. \quad (5)$$

The expression (4) can then be written in a form:

$$W_{0 \rightarrow 1} = \sum_{i,j} c_i c_j^* \langle \Psi_0 | \langle P_{i,j}(t) \rangle_0 | \Psi_0 \rangle. \quad (6)$$

Thus, the probability of transition from the eigenstate $|n\rangle$ to the eigenstate $|m\rangle$ can be calculated by using the corresponding matrix element of the transition operator $P_{m,m}$ averaged over photon vacuum:

$$W_{n \rightarrow m} = \langle n | \langle P_{m,m}(t) \rangle_0 | n \rangle. \quad (7)$$

It follows from the completeness of the qubits states $|i\rangle$ that the sum of diagonal elements of the transition operator is equal to one:

$$\sum_i P_{i,i} = 1. \quad (8)$$

As follows from the definition (5), the expression for the elements of the transition operator satisfy the Heisenberg equation:

$$\frac{d}{dt} P_{i,j}(t) = i [H, P_{i,j}(t)], \quad (9)$$

with the initial conditions $P_{i,j}(0) = |i\rangle \langle j|$.

Unlike the equations for spin operators or elements of the density matrix, equations for $P_{i,j}$ are linear: they contain only the first degrees of the same operators. The number of equations for the transition operator is determined by the number of states from the complete set. For example, for one qubit there are only two states, the excited state $|e\rangle$ and the ground state $|g\rangle$. Accordingly, there are four matrix elements of the transition operator: P_{ee} , P_{gg} , P_{eg} , and P_{ge} . However, there are only three independent equations since the P_{eg} is a complex conjugate to a P_{ge} . For two qubits there are four states and, consequently, there are ten independent equations: four equations for the diagonal elements of the transition operator and six equations for off-diagonal ones (excluding complex conjugates).

In general case, the matrix elements of the transition operator averaged over photon vacuum have the following form:

$$\langle P_{i,j}(t) \rangle_0 = \sum_{m,n} c_{mn}^{ij}(t) |m\rangle \langle n|, \quad (10)$$

where $c_{mn}^{ij}(t)$ are c-numbers.

In principle, we may choose the basis states of a spin system in the following way:

$$\langle P_{i,j}(t) \rangle_0 = \sum_{m,n} c_{mn}^{ij}(t) |m\rangle \langle n|; \quad i \neq j; \quad m \neq n \quad (11)$$

$$\langle P_{i,i}(t) \rangle_0 = \sum_q c_q^i(t) |q\rangle \langle q| \quad (12)$$

In this case, the off-diagonal element, Eq. 11, of transition operator provides the transitions between different states of a spin system, while the diagonal element of transition operator has only diagonal matrix elements in the Hilbert space of a spin system.

By the definition, the qubit density matrix of a spin system, $\rho_{S,j_i}(t) = \langle j | Tr_\nu [\rho(t)] | i \rangle \equiv \langle j | \rho_S(t) | i \rangle$, where $\rho(t)$ is the density matrix of the whole system:

$$\rho(t) = e^{-iHt} \rho(0) e^{iHt}, \quad (13)$$

can be expressed in terms of the average value of the transition operator:

$$\rho_{S,j_i}(t) = Tr_{S,\nu} (\rho(0) P_{i,j}(t)) \equiv \langle P_{i,j}(t) \rangle, \quad (14)$$

where the trace is taken over both the qubit system and the photon field, and $\rho(0)$ is the initial density matrix of the whole system.

If we assume that initially the field is in a photon vacuum:

$$\rho(0) = \rho_S(0) \otimes \rho_\nu(0) = \rho_S(0) \otimes |0\rangle \langle 0|, \quad (15)$$

we then obtain from (14):

$$\langle l | \rho_S(t) | m \rangle = \sum_{n,q} \langle n | \rho_S(0) | q \rangle \langle q | \langle P_{m,l}(t) \rangle_0 | n \rangle. \quad (16)$$

Therefore, the matrix elements of a reduced density matrix can be expressed in terms of the matrix elements of the vacuum average of the transition operator if the initial density matrix $\rho_S(0)$ is known. It should be noted that in contrast to the elements of the density matrix, which are numerical functions, the matrix elements of $P_{i,j}(t)$ are the operator functions. If the system is initially in one of its basis states $|s\rangle$ ($\langle s | \rho_S(0) | s \rangle = 1$), then it follows from (15):

$$\langle l | \rho_S(t) | m \rangle = \langle s | \langle P_{m,l}(t) \rangle_0 | s \rangle \quad (17)$$

For basis set with the properties (11) and (12) it follows from (17) that the off-diagonal elements of reduced density matrix are zero. For the diagonal elements of reduced density matrix, that is, for the populations, we obtain:

$$\langle m | \rho_S(t) | m \rangle = \langle s | \langle P_{m,m}(t) \rangle_0 | s \rangle \quad (18)$$

Therefore, if $m \neq s$ the population $\langle m | \rho_S(t) | m \rangle$ can be understood as the transition amplitude from the initial state $|s\rangle$ to the state $|m\rangle$.

III. MULTI-QUBIT SYSTEM

Consider a system consisting of N qubits in a one-dimensional infinite waveguide. This system can be described by a Jaynes-Cummings Hamiltonian:

$$H = \frac{1}{2} \sum_{n=1}^N \left(1 + \sigma_z^{(n)}\right) \Omega_n + \sum_k \omega_k a_k^\dagger a_k + \sum_k \left(a_k^\dagger S_k^- + S_k^+ a_k \right), \quad (19)$$

where we introduced collective atomic spin operators:

$$S_k^- = \sum_{n=1}^N g_k^{(n)} e^{-ikx_n} \sigma_-^{(n)}, \quad S_k^+ = \sum_{n=1}^N g_k^{*(n)} e^{ikx_n} \sigma_+^{(n)}, \quad (20)$$

Here $\sigma_z^{(n)}$ is a Pauli spin operator, Ω_n is a resonant frequency of n th qubit, $a_k^\dagger(a_k)$ are creation (annihilation) operators for a k mode photon, ω_k is a photon frequency, $\sigma_-^{(n)} = |g\rangle_{nn} \langle e|$ and $\sigma_+^{(n)} = |e\rangle_{nn} \langle g|$ are the atomic ladder operators which lower or raise a state of the n th qubit, g_k is a coupling strength between the qubit and the field, x_n is a spatial coordinate of the n th qubit.

From (9) and (19) we obtain the equation of motion for the transition operator:

$$\begin{aligned} \frac{d}{dt} P_{ij} = & \\ & \frac{i}{2} \sum_{n=1}^N \Omega_n \left(e^{iHt} \sigma_Z^{(n)} |i\rangle \langle j| e^{-iHt} - e^{iHt} |i\rangle \langle j| \sigma_Z^{(n)} e^{-iHt} \right) \\ & + i \sum_k a_k^\dagger(t) \left(e^{iHt} S_k^- |i\rangle \langle j| e^{-iHt} - e^{iHt} |i\rangle \langle j| S_k^- e^{-iHt} \right) \\ & + i \sum_k \left(e^{iHt} S_k^+ |i\rangle \langle j| e^{-iHt} - e^{iHt} |i\rangle \langle j| S_k^+ e^{-iHt} \right) a_k(t), \end{aligned} \quad (21)$$

where the photon operators are in the Heisenberg representation:

$$a_k^\dagger(t) = e^{iHt} a_k^\dagger e^{-iHt}, \quad a_k(t) = e^{iHt} a_k e^{-iHt}. \quad (22)$$

For photon operators the equations of motion are as follows:

$$i \frac{da_k}{dt} = [a_k(t), H] = \omega_k a_k(t) + S_k^-(t), \quad (23a)$$

$$i \frac{da_k^\dagger}{dt} = [a_k^\dagger(t), H] = -\omega_k a_k^\dagger(t) - S_k^+(t). \quad (23b)$$

where $S_k^\pm(t)$ are collective spin operators in the Heisenberg picture. The formal solution of these equations is given by:

$$a_k(t) = a_k(0) e^{-i\omega_k t} - i \int_0^t e^{-i\omega_k(t-\tau)} S_k^-(\tau) d\tau, \quad (24a)$$

$$a_k^\dagger(t) = a_k^\dagger(0) e^{i\omega_k t} + i \int_0^t e^{i\omega_k(t-\tau)} S_k^+(\tau) d\tau. \quad (24b)$$

where the first term in the right hand side of (24) is a free field part and the second term is a part radiated by atoms.

Since we considering a 1D waveguide, k takes only two directions, $k = \pm|k| = \pm\omega/v_g$. From (20) it follows that positive k , $|k| = +\omega/v_g$, corresponds to the right (forward) propagating modes, while the negative k , $|k| = -\omega/v_g$, corresponds to the left (backward) propagating modes. Therefore, the operators $a_{+|k|}, a_{+|k|}^\dagger$, and $a_{-|k|}, a_{-|k|}^\dagger$ correspond to right and left propagating photons, respectively.

Even though the photon operators $a_k^\dagger(t), a_k(t)$ commute with collective spin operators $S_k^\pm(t)$, each term in (24) does not commute with $S_k^\pm(t)$. This explains the position of these operators in the third term of Hamiltonian (19). They should be placed in such a way that in the final expression the creation operators $a_k^\dagger(t)$ were placed on the left of the transition operator $P_{i,j}$, while the annihilation operators $a_k(t)$ were placed on the right. This is necessary for the terms with initial photons to be dropped out upon averaging the transition operator over the photon vacuum.

Substituting the expressions (24) into the equation of motion (21) we obtain:

$$\begin{aligned}
\frac{dP_{ij}}{dt} &= i\frac{1}{2} \sum_{n=1}^N \Omega_n \left(e^{iHt} \sigma_Z^{(n)} |i\rangle \langle j| e^{-iHt} - e^{iHt} |i\rangle \langle j| \sigma_Z^{(n)} e^{-iHt} \right) \\
&+ i \sum_k a_k^\dagger(0) e^{i\omega_k t} e^{iHt} S_k^- |i\rangle \langle j| e^{-iHt} - i \sum_k a_k^\dagger(0) e^{i\omega_k t} e^{iHt} |i\rangle \langle j| S_k^- e^{-iHt} \\
&+ i \sum_k e^{iHt} S_k^+ |i\rangle \langle j| e^{-iHt} a_k(0) e^{-i\omega_k t} - i \sum_k e^{iHt} |i\rangle \langle j| S_k^+ e^{-iHt} a_k(0) e^{-i\omega_k t} \\
&+ \sum_k \int_0^t e^{i\omega_k(t-\tau)} S_k^+(\tau) d\tau e^{iHt} [|i\rangle \langle j|, S_k^-] e^{-iHt} + \sum_k e^{iHt} [S_k^+, |i\rangle \langle j|] e^{-iHt} \int_0^t e^{-i\omega_k(t-\tau)} S_k^-(\tau) d\tau
\end{aligned} \tag{25}$$

Here we write the equation in such a manner that the action of atomic operators on system states is clearly visible. Equation (25) can be rewritten in terms of transition operators and atomic operators in the Heisenberg picture, since $e^{iHt} \sigma_Z^{(n)} |i\rangle \langle j| e^{-iHt} = \sigma_Z^{(n)}(t) P_{i,j}(t)$ (the same procedure applies to the terms with S_k^\pm as well).

Up to now, we did not make any approximations: the above expressions are exact. In order to solve the equation (25), the following assumptions are made:

$$\sigma_-^{(n)}(\tau) \approx \sigma_-^{(n)}(t) e^{-i\Omega_n(\tau-t)}, \tag{26a}$$

$$\sigma_+^{(n)}(\tau) \approx \sigma_+^{(n)}(t) e^{i\Omega_n(\tau-t)}. \tag{26b}$$

Assuming that all qubit frequencies are identical and equal to some value Ω , we then obtain:

$$S_k^-(\tau) \approx S_k^-(t) e^{-i\Omega(\tau-t)}, \tag{27a}$$

$$S_k^+(\tau) \approx S_k^+(t) e^{i\Omega(\tau-t)}. \tag{27b}$$

The assumptions (26), (27) are equivalent to Wigner-Weisskopf or Markov approximations [9, 27]. It allows

us to take $S_k^\pm(\tau)$ out of the integrand in the last line of (25). We then rewrite the rest of the integrals by taking into account the resonant approximation, i.e. assuming that the main contribution to the integral is near the resonance frequency Ω . This allows us to take the upper limit to infinity, and we get:

$$\begin{aligned}
\int_0^t e^{i(\omega-\Omega)(t-t')} dt' &\approx \int_0^\infty e^{i(\omega-\Omega)\tau} d\tau = \\
&\pi\delta(\omega-\Omega) + i P.v. \left(\frac{1}{\omega-\Omega} \right), \tag{28}
\end{aligned}$$

where $\delta(\omega)$ is a Dirac delta function and $P.v.$ is a Cauchy principal value.

According to all assumptions above, we obtain from (25) the equation of motion for the transition operator in the following form:

$$\begin{aligned}
\frac{dP_{ij}}{dt} &= i\frac{1}{2} \sum_{n=1}^N \Omega_n \left(e^{iHt} \sigma_Z^{(n)} |i\rangle \langle j| e^{-iHt} - e^{iHt} |i\rangle \langle j| \sigma_Z^{(n)} e^{-iHt} \right) \\
&+ i \sum_k a_k^\dagger(0) e^{i\omega_k t} e^{iHt} [S_k^-, |i\rangle \langle j|] e^{-iHt} + i \sum_k e^{iHt} [S_k^+, |i\rangle \langle j|] e^{-iHt} a_k(0) e^{-i\omega_k t} \\
&+ \sum_{n,m} \frac{\Gamma_{n,m}}{2} e^{iHt} \left(2\sigma_+^{(m)} |i\rangle \langle j| \sigma_-^{(n)} - \sigma_+^{(m)} \sigma_-^{(n)} |i\rangle \langle j| - |i\rangle \langle j| \sigma_+^{(m)} \sigma_-^{(n)} \right) e^{-iHt} \\
&+ i \sum_{n,m} \alpha_{n,m} e^{iHt} \left(|i\rangle \langle j| \sigma_+^{(m)} \sigma_-^{(n)} - \sigma_+^{(m)} \sigma_-^{(n)} |i\rangle \langle j| \right) e^{-iHt}
\end{aligned} \tag{29}$$

where according to the Fermi Golden rule we have intro-

duced a decay rate $\Gamma_{n,m}$:

$$\Gamma_{n,m} = \sum_k 2\pi\delta(\omega_k - \Omega) g_k^{(n)} g_k^{*(m)} e^{-ik(x_n - x_m)}, \tag{30}$$

and a frequency shift $\alpha_{n,m}$:

$$\alpha_{n,m} = \sum_k g_k^{(n)} g_k^{*(m)} e^{-ik(x_n - x_m)} P.v. \left(\frac{1}{\omega_k - \Omega} \right). \quad (31)$$

Equation (29) is the most general case of the equation of motion for the matrix elements of the transition operator (5) for N qubits with identical resonant frequencies. When equation (29) is averaged over the initial photon vacuum, the second line in (29) can be dropped out.

For a long 1D waveguide we can replace the summation over k by the integration:

$$\sum_k f(k) \rightarrow \frac{L}{2\pi} \int_{-\infty}^{+\infty} f(k) d|k| = \frac{L}{\pi v_g} \int_0^{\infty} (f(|k|) + f(-|k|)) d\omega \quad (32)$$

where L is the quantization length in the propagation direction and v_g is the photon group velocity.

If we assume that the coupling strength is the same for all qubits, $g_k^{(n)} = g_k^{(m)} \equiv g_k$ and is symmetrical, i.e. $g_k = g_{-k}$, and it contributes mainly near the resonance $g_k \approx g_{k_0}$, where $k_0 = \Omega/v_g$, we then obtain for (30) and (31):

$$\Gamma_{n,m} = \Gamma \cos(k_0 |d_{n,m}|), \quad (33a)$$

$$\alpha_{n,m} = -\frac{\Gamma}{2} \sin(k_0 |d_{n,m}|), \quad (33b)$$

where $d_{n,m} = (x_n - x_m)$ is the distance between n th and m th qubit, Γ is the single-qubit emission rate into the waveguide mode:

$$\Gamma = \frac{2L}{v_g} |g_{k_0}|^2, \quad (34)$$

The expression (33a) is obtained with the help of the following relation:

$$P.v. \int_0^{+\infty} \frac{\cos(\omega d_{n,m}/v_g)}{\omega - \Omega} d\omega = -\pi \sin(k_0 |d_{n,m}|). \quad (35)$$

The expression (35) is exact if counter-rotating terms in the qubit-field interaction is taken into account (Suppl. in [35]). Nevertheless, within a rotating wave approximation the Eq. 35 provides a good accuracy for $d > \lambda/4$ [21].

The quantities $\Gamma_{n,m}$ and $\alpha_{n,m}$ denote the dissipative and coherent interaction rates, respectively. The coherent interaction results from the exchange of virtual photons between qubits at all continuum frequencies except for a single frequency $\omega = \Omega$. It gives rise to the shift of the qubit frequencies. In contrast to the case of a free space, these inter-qubit interactions have an infinite range. In addition, the interaction between any two qubits can be easily switched off by a proper choice of the value $k_0 |d_{n,m}|$. In the simple case for which a distance between any two neighbor qubits is d , the coherent inter qubit interaction vanish if $k_0 d = n\pi$ where n is any positive integer.

IV. RADIATION SPECTRUM AND CALCULATION OF THE CORRELATION FUNCTIONS

In circuit quantum electrodynamics it is possible to experimentally measure both the full photon spectrum $\langle a_k^\dagger(t) a_k(t) \rangle$ and one-time mean values of single-photon operators $\langle a_k(t) \rangle$, $\langle a_k^\dagger(t) \rangle$ [36, 37]. Moreover, we can construct more complex photon correlation functions with a higher order of photon operators and experimentally measure them as well [38]. In this paper, the main attention is paid to the quantity $\langle a_k^\dagger(t) a_k(t) \rangle$ which defines the photon radiation spectrum.

From the expressions for photon operators (24) we obtain:

$$\langle a_k^\dagger(t) a_k(t) \rangle = \int_0^t d\tau \int_0^t d\tau' e^{-i\omega_k(\tau - \tau')} \langle S_k^+(\tau) S_k^-(\tau') \rangle. \quad (36)$$

From (36) we obtain the total photon emission rate, that is, the rate of the energy loss:

$$W(t) = \frac{d}{dt} \sum_k \langle a_k^\dagger(t) a_k(t) \rangle = \langle S_k^+(t) S_k^-(t) \rangle \quad (37)$$

The frequency dependent photon radiation spectrum is defined as the limit of (36) when t tends to infinity:

$$S(\omega_k) = \int_0^{\infty} d\tau \int_0^{\infty} d\tau' e^{-i\omega_k(\tau - \tau')} \langle S_k^+(\tau) S_k^-(\tau') \rangle. \quad (38)$$

The averaging in above equations is understood as the tracing over both the states S of a spin system and the states ν of a photon field.

$$\langle S_k^+(\tau) S_k^-(\tau') \rangle = Tr_{S,\nu} (S_k^+(\tau) S_k^-(\tau') \rho(0)) \quad (39)$$

where $\rho(0)$ is the initial density matrix of the whole system.

From definition (20) we obtain:

$$\langle S_k^+(\tau) S_k^-(\tau') \rangle = \sum_{n,m}^N g_k^{(m)} g_k^{*(n)} e^{ik(x_n - x_m)} \langle \sigma_+^{(n)}(\tau) \sigma_-^{(m)}(\tau') \rangle. \quad (40)$$

The expression for two-time correlation function $\langle \sigma_+^{(n)}(\tau) \sigma_-^{(m)}(\tau') \rangle$ can be written in two ways depending on the relation between τ and τ' . If $\tau > \tau'$, then:

$$\langle \sigma_+^{(n)}(\tau) \sigma_-^{(m)}(\tau') \rangle = Tr_{S,\nu} \left[\rho(\tau') \sigma_+^{(n)}(\tau - \tau') \sigma_-^{(m)}(0) \right]. \quad (41a)$$

If $\tau < \tau'$, then:

$$\left\langle \sigma_+^{(n)}(\tau) \sigma_-^{(m)}(\tau') \right\rangle = Tr_{S,\nu} \left[\sigma_+^{(m)}(0) \sigma_-^{(n)}(\tau' - \tau) \rho(\tau) \right]. \quad (41b)$$

These prescriptions come from the requirement for the time argument of a spin operator to be always positive.

The expressions (41) are exact. If we assume the system is always in a photon vacuum state (15) we obtain for (41a), (41b):

$$\begin{aligned} \left\langle \sigma_+^{(n)}(\tau) \sigma_-^{(m)}(\tau') \right\rangle &= \\ Tr_S \left[\rho_S(\tau') \left\langle \sigma_+^{(n)}(\tau - \tau') \right\rangle_0 \sigma_-^{(m)}(0) \right], & \tau > \tau' \end{aligned} \quad (42a)$$

$$\begin{aligned} \left\langle \sigma_+^{(n)}(\tau) \sigma_-^{(m)}(\tau') \right\rangle &= \\ Tr_S \left[\sigma_+^{(m)}(0) \left\langle \sigma_-^{(n)}(\tau' - \tau) \right\rangle_0 \rho_S(\tau) \right], & \tau < \tau' \end{aligned} \quad (42b)$$

With the aid of (16) we can rewrite the density matrix $\rho_S(t)$ in (42) in terms of the initial density matrix $\rho_S(0)$ and transition operators:

$$\left\langle \sigma_+^{(n)}(\tau) \sigma_-^{(m)}(\tau') \right\rangle_+ = \sum_{l,q} \sum_{s,p} \langle s | \rho_S(0) | p \rangle \langle p | \langle P_{q,l}(\tau') \rangle_0 | s \rangle \langle q | \left\langle \sigma_+^{(n)}(\tau - \tau') \right\rangle_0 \sigma_-^{(m)}(0) | l \rangle, \quad \tau > \tau' \quad (43a)$$

$$\left\langle \sigma_+^{(n)}(\tau) \sigma_-^{(m)}(\tau') \right\rangle_- = \sum_{l,q} \sum_{s,p} \langle l | \sigma_+^{(n)}(0) \left\langle \sigma_-^{(m)}(\tau' - \tau) \right\rangle_0 | q \rangle \langle s | \rho_S(0) | p \rangle \langle p | \langle P_{l,q}(\tau) \rangle_0 | s \rangle. \quad \tau < \tau' \quad (43b)$$

Here plus and minus subscript just indicate the positive and negative time difference. The quantity $\left\langle \sigma_{\pm}^{(n)}(\tau - \tau') \right\rangle_0$ in (43), which refers to the individual nth spin of a system should be expressed in terms of the matrix elements of transition operator acting in the collective basis set of a spin system.

Putting all things together, we have the following expression for spectrum (36):

$$\begin{aligned} \left\langle a_k^\dagger(t) a_k(t) \right\rangle &= \sum_{n,m} g_k^{(m)} g_k^{*(n)} e^{ik(x_n - x_m)} \int_0^t d\tau \int_0^\tau d\tau' e^{-i\omega_k(\tau - \tau')} \left\langle \sigma_+^{(n)}(\tau) \sigma_-^{(m)}(\tau') \right\rangle_+ \\ &+ \sum_{n,m} g_k^{(m)} g_k^{*(n)} e^{ik(x_n - x_m)} \int_0^t d\tau \int_\tau^t d\tau' e^{-i\omega_k(\tau - \tau')} \left\langle \sigma_+^{(n)}(\tau) \sigma_-^{(m)}(\tau') \right\rangle_- \end{aligned} \quad (44)$$

where two-time correlation functions are given in (43) for different time intervals. Therefore, we can calculate the desired correlation functions using only transition operators averaged over the vacuum field.

Note that this approach allows one to calculate not only two-time correlation functions similar to (41) but more complex ones as well. In (43) we reduce the averaged value of two operators to an average of one operator multiplied by the second operator at zero time. The same principle can be used to reduce, say, a four-time correlation function to a three-time correlation function, which can be also reduced the same way to a two-time correlation function, and so on. Thus, we can find higher-order correlation functions using only transition operators found from (29).

V. TRANSITION OPERATORS FOR TWO-QUBIT SYSTEM

For two-qubit system there are four basis states:

$$|1\rangle = |gg\rangle; \quad |2\rangle = |ee\rangle; \quad |3\rangle = |ge\rangle; \quad |4\rangle = |eg\rangle \quad (45)$$

However, we use here a so called Dicke basis consisting of states $|1\rangle$, $|2\rangle$ and symmetrical and asymmetrical superposition of states $|3\rangle$ and $|4\rangle$:

$$\begin{aligned} |G\rangle &= |gg\rangle, \quad |E\rangle = |ee\rangle, \\ |S\rangle &= \frac{1}{\sqrt{2}} (|ge\rangle + |eg\rangle), \quad |A\rangle = \frac{1}{\sqrt{2}} (|ge\rangle - |eg\rangle). \end{aligned} \quad (46)$$

The advantage of basis states (46) over the (45) is that the equations of motion for diagonal matrix elements of transition operator are independent of the off-diagonal ones.

Using the definition of lowering and raising operators for the regular basis (45), it is easy to show how they act on the new basis states (46):

$$\begin{aligned}\sigma_+^{(1,2)} |G\rangle &= \frac{1}{\sqrt{2}} (|S\rangle \mp |A\rangle), & \sigma_-^{(1,2)} |G\rangle &= 0, \\ \sigma_+^{(1,2)} |E\rangle &= 0, & \sigma_-^{(1,2)} |E\rangle &= \frac{1}{\sqrt{2}} (|S\rangle \pm |A\rangle), \\ \sigma_+^{(1,2)} |S\rangle &= \frac{1}{\sqrt{2}} |E\rangle, & \sigma_-^{(1,2)} |S\rangle &= \frac{1}{\sqrt{2}} |G\rangle, \\ \sigma_+^{(1,2)} |A\rangle &= \pm \frac{1}{\sqrt{2}} |E\rangle, & \sigma_-^{(1,2)} |A\rangle &= \mp \frac{1}{\sqrt{2}} |G\rangle.\end{aligned}\quad (47a)$$

$$(47b)$$

The same can be easily done for Pauli spin operators:

$$\begin{aligned}\sigma_Z^{(1,2)} |G\rangle &= -|G\rangle, & \sigma_Z^{(1,2)} |E\rangle &= |E\rangle, \\ \sigma_Z^{(1,2)} |A\rangle &= \mp |S\rangle, & \sigma_Z^{(1,2)} |S\rangle &= \mp |A\rangle.\end{aligned}\quad (48)$$

Next, we apply the equation (29) for $N = 2$ and assume for the decay rates, $\Gamma_{11} = \Gamma_{22} = \Gamma$, $\Gamma_{12} = \Gamma_{21} = \Gamma \cos(k_0 d)$, and for the frequency shifts $\alpha_{11} = \alpha_{22} = 0$, $\alpha_{12} = \alpha_{21} = \Gamma \sin(k_0 d)/2$, where d is the distance between two qubits. By averaging the equation (29) over the photon vacuum state $|0\rangle$, the terms including photon operators in the second line in (29) will be dropped out, and we can obtain equations for the matrix elements of the transition operator. For the basis (46) we have sixteen equations in total, but since the off-diagonal transition operators $P_{i,j}$ is a hermitian conjugate of $P_{j,i}$, it is sufficient to find the solution only for ten matrix elements of the transition operator. For the diagonal matrix elements of transition operator (which we will refer to as populations by analogy with diagonal elements of density matrix), we find:

$$\frac{d\langle P_{EE}\rangle_0}{dt} = -2\Gamma \langle P_{EE}\rangle_0, \quad (49a)$$

$$\frac{d\langle P_{SS}\rangle_0}{dt} = \Gamma (1 + \cos k_0 d) (\langle P_{EE}\rangle_0 + \langle P_{SS}\rangle_0), \quad (49b)$$

$$\frac{d\langle P_{AA}\rangle_0}{dt} = \Gamma (1 - \cos k_0 d) (\langle P_{EE}\rangle_0 - \langle P_{AA}\rangle_0), \quad (49c)$$

$$\begin{aligned}\frac{d\langle P_{GG}\rangle_0}{dt} &= \Gamma (1 + \cos k_0 d) \langle P_{SS}\rangle_0 \\ &+ \Gamma (1 - \cos k_0 d) \langle P_{AA}\rangle_0.\end{aligned}\quad (49d)$$

For the off-diagonal matrix elements of the transition operator (which we will refer to as coherences) we obtain:

$$\frac{d\langle P_{GE}\rangle_0}{dt} = -(2i\Omega + \Gamma) \langle P_{GE}\rangle_0, \quad (50a)$$

$$\frac{d\langle P_{AS}\rangle_0}{dt} = -\Gamma (1 + i \sin k_0 d) \langle P_{AS}\rangle_0, \quad (50b)$$

$$\begin{aligned}\frac{d\langle P_{AE}\rangle_0}{dt} &= -i \left(\Omega + \frac{\Gamma}{2} \sin k_0 d \right) \langle P_{AE}\rangle_0 \\ &- \frac{\Gamma}{2} (3 - \cos k_0 d) \langle P_{AE}\rangle_0,\end{aligned}\quad (50c)$$

$$\begin{aligned}\frac{d\langle P_{SE}\rangle_0}{dt} &= -i \left(\Omega - \frac{\Gamma}{2} \sin k_0 d \right) \langle P_{SE}\rangle_0 \\ &- \frac{\Gamma}{2} (3 + \cos k_0 d) \langle P_{SE}\rangle_0,\end{aligned}\quad (50d)$$

$$\begin{aligned}\frac{d\langle P_{GA}\rangle_0}{dt} &= -i \left(\Omega - \frac{\Gamma}{2} \sin k_0 d \right) \langle P_{GA}\rangle_0 \\ &- \Gamma (1 - \cos k_0 d) \langle P_{AE}\rangle_0 - \frac{\Gamma}{2} (1 - \cos k_0 d) \langle P_{GA}\rangle_0,\end{aligned}\quad (50e)$$

$$\begin{aligned}\frac{d\langle P_{GS}\rangle_0}{dt} &= -i \left(\Omega + \frac{\Gamma}{2} \sin k_0 d \right) \langle P_{GS}\rangle_0 \\ &+ \Gamma (1 + \cos k_0 d) \langle P_{SE}\rangle_0 - \frac{\Gamma}{2} (1 + \cos k_0 d) \langle P_{GS}\rangle_0.\end{aligned}\quad (50f)$$

Thus in the basis (46), the equations for populations are decoupled from those for the coherences. Moreover, first four equations for the coherences are fully independent and related only to their corresponding matrix elements. These equations can be solved without any problems since the initial conditions, which are based on the definition of transition operator (5), are always unique: $P_{ij}(0) = |i\rangle \langle j|$.

By solving two groups of equations we find all matrix elements for the transition operator for a two-qubit system in an open waveguide. For the populations we obtain the following solutions:

$$\langle P_{EE}(t)\rangle_0 = e^{-2\Gamma t} |E\rangle \langle E|, \quad (51a)$$

$$\begin{aligned}\langle P_{SS}(t)\rangle_0 &= |S\rangle \langle S| e^{-\Gamma+t} \\ &- \frac{1 + \cos k_0 d}{1 - \cos k_0 d} (e^{-2\Gamma t} - e^{-\Gamma+t}) |E\rangle \langle E|,\end{aligned}\quad (51b)$$

$$\begin{aligned}\langle P_{AA}(t)\rangle_0 &= |A\rangle \langle A| e^{-\Gamma-t} \\ &- \frac{1 - \cos k_0 d}{1 + \cos k_0 d} (e^{-2\Gamma t} - e^{-\Gamma-t}) |E\rangle \langle E|,\end{aligned}\quad (51c)$$

$$\begin{aligned}\langle P_{GG}(t)\rangle_0 &= |G\rangle \langle G| \\ &- (e^{-\Gamma+t} - 1) |S\rangle \langle S| - (e^{-\Gamma-t} - 1) |A\rangle \langle A| \\ &+ \frac{(1 + \cos k_0 d)^2}{1 - \cos k_0 d} \left[\frac{(e^{-2\Gamma t} - 1)}{2} - \frac{(e^{-\Gamma+t} - 1)}{1 + \cos k_0 d} \right] |E\rangle \langle E| \\ &+ \frac{(1 - \cos k_0 d)^2}{1 + \cos k_0 d} \left[\frac{(e^{-2\Gamma t} - 1)}{2} - \frac{(e^{-\Gamma-t} - 1)}{1 - \cos k_0 d} \right] |E\rangle \langle E|.\end{aligned}\quad (51d)$$

For coherences we obtain:

$$\langle P_{GE}(t) \rangle_0 = e^{-(2i\Omega + \Gamma)t} |G\rangle \langle E|, \quad (52a)$$

$$\langle P_{AS}(t) \rangle_0 = e^{-\Gamma(1+i\sin(k_0d))t} |A\rangle \langle S|, \quad (52b)$$

$$\langle P_{AE}(t) \rangle_0 = e^{-(i\Omega_+ + \frac{\Gamma_-}{2} + \Gamma)t} |A\rangle \langle E|, \quad (52c)$$

$$\langle P_{SE}(t) \rangle_0 = e^{-(i\Omega_- + \frac{\Gamma_+}{2} + \Gamma)t} |S\rangle \langle E|, \quad (52d)$$

$$\begin{aligned} \langle P_{GA}(t) \rangle_0 &= e^{-(i\Omega_- + \frac{\Gamma_-}{2})t} |G\rangle \langle A| + \\ &\frac{1 - \cos k_0d}{1 + i \sin k_0d} \left(e^{-(i\Omega_+ + \frac{\Gamma_-}{2} + \Gamma)t} - e^{-(i\Omega_- + \frac{\Gamma_-}{2})t} \right) |A\rangle \langle E|, \end{aligned} \quad (52e)$$

$$\begin{aligned} \langle P_{GS}(t) \rangle_0 &= e^{-(i\Omega_+ + \frac{\Gamma_+}{2})t} |G\rangle \langle S| - \\ &\frac{1 + \cos k_0d}{1 - i \sin k_0d} \left(e^{-(i\Omega_- + \frac{\Gamma_+}{2} + \Gamma)t} - e^{-(i\Omega_+ + \frac{\Gamma_+}{2})t} \right) |S\rangle \langle E|. \end{aligned} \quad (52f)$$

Here for simplification, we introduce the shifted resonant frequencies and modified decay rates:

$$\Omega_+ = \Omega + \frac{\Gamma}{2} \sin k_0d; \quad \Omega_- = \Omega - \frac{\Gamma}{2} \sin k_0d; \quad (53a)$$

$$\Gamma_+ = \Gamma(1 + \cos k_0d); \quad \Gamma_- = \Gamma(1 - \cos k_0d); \quad (53b)$$

which depend on the effective distance between the qubits.

Unlike the usual solution for the density matrix, expressions (51) and (52) are the operator functions. Nevertheless, knowing the expressions for the matrix elements of the transition operator, we can easily find the density matrix using relations (14) or (15).

VI. TRANSITION PROBABILITIES FOR TWO QUBITS

As was noted in Sec.2, the probability of a system to transit from one state to another can be found with the aid of transition operators (see Eq. 7). Here we calculate the probabilities which contribute to the total rate of superradiant emission which will be given below in Sec. 7.

For both qubits initially in an excited state $|\Psi_0\rangle = |ee\rangle = |E\rangle$ we can find the probability that at time t the system remains in the initial state:

$$W_{E \rightarrow E} = \langle E | P_{EE} | E \rangle = e^{-2\Gamma t}. \quad (54)$$

The probabilities for both qubits to decay to symmetric and asymmetric state are as follows:

$$\begin{aligned} W_{E \rightarrow S} &= \langle E | P_{SS} | E \rangle = \\ &= \frac{1 + \cos k_0d}{1 - \cos k_0d} \left(e^{-2\Gamma t} - e^{-\Gamma(1 + \cos k_0d)t} \right). \end{aligned} \quad (55)$$

$$\begin{aligned} W_{E \rightarrow A} &= \langle E | P_{AA} | E \rangle = \\ &= \frac{1 - \cos k_0d}{1 + \cos k_0d} \left(e^{-2\Gamma t} - e^{-\Gamma(1 - \cos k_0d)t} \right). \end{aligned} \quad (56)$$

When qubits are initially in a symmetric, $|\Psi_0\rangle = (|ge\rangle + |eg\rangle)/\sqrt{2} = |S\rangle$, or asymmetric, $|\Psi_0\rangle = (|ge\rangle - |eg\rangle)/\sqrt{2} = |A\rangle$ states, the probabilities of the system to remain in the initial states are given by:

$$W_{S \rightarrow S} = \langle S | P_{SS} | S \rangle = e^{-\Gamma(1 + \cos k_0d)t}. \quad (57)$$

$$W_{A \rightarrow A} = \langle A | P_{AA} | A \rangle = e^{-\Gamma(1 - \cos k_0d)t} \quad (58)$$

As is clear from (51b) and (51c) the transitions between symmetric and asymmetric states are forbidden:

$$W_{A \rightarrow S} = \langle A | P_{SS} | A \rangle = 0; \quad W_{S \rightarrow A} = \langle S | P_{AA} | S \rangle = 0 \quad (59)$$

Therefore, the $|A\rangle$ and $|S\rangle$ states are completely decoupled from each other no matter what is the value of k_0d .

The symmetric and asymmetric states have different decay rates which depend on the value of k_0d . As is seen from (57), (58) for a given value of k_0d the decay rate for the state $|S\rangle$ is always greater than that for the state $|A\rangle$. In addition, for $k_0d = 2n\pi$, where n is a positive integer or 0, the population of the $|A\rangle$ remains constant ($W_{A \rightarrow A} = 1$). In this case, the state $|A\rangle$ is called the dark state since it does not interact with the electromagnetic field, while the state $|S\rangle$ is called a bright state. If $k_0d = (2n+1)\pi$ the situation is reversed: the state $|S\rangle$ becomes a dark state, while the state $|A\rangle$ becomes a bright state.

Finally, for the calculation of $W(t)$ we will need the off-diagonal matrix elements:

$$\langle A | \langle P_{AS}(t) \rangle_0 | S \rangle = e^{-\Gamma(1+i\sin(k_0d))t} \quad (60)$$

The transitions (55, 56) depend on the effective distance between the qubits k_0d . For example, for $k_0d = \pi/2$ there are equal probabilities of transitions to symmetric and asymmetric states, $W_{E \rightarrow S} = W_{E \rightarrow A} = e^{-2\Gamma t} - e^{-\Gamma t}$.

We should separately consider the case when $k_0d = n\pi$. For this case, both the numerator and denominator in (55) and (56) tend to zero. A correct solution can be obtained if we put $k_0d = n\pi$ directly in the equations (49b) and (49c), or by expanding $\cos(k_0d)$ near $k_0d \approx n\pi + \epsilon$ where ϵ is a small value. Both approaches give the same result. For $k_0d = 2n\pi$ we obtain the following transition probabilities:

$$W_{E \rightarrow S} = 2\Gamma t e^{-2\Gamma t}, \quad W_{E \rightarrow A} = 0 \quad (61)$$

As it is clearly seen from (61), for an even number of $n = 0, 2, 4 \dots$, the transition from state $|E\rangle$ to asymmetric entangled state $|A\rangle$ is forbidden. For an odd number of $n = 1, 3 \dots$ the situation is reversed: the transition to symmetric state is now forbidden, and for transition to asymmetric state we get the relation $W_{E \rightarrow A} = 2\Gamma t e^{-2\Gamma t}$.

VII. SUPERRADIANT SPECTRA OF TWO QUBITS IN A WAVEGUIDE

Now we switch to the calculation of radiation spectrum for a two-qubit system. As was shown in (36), the spectrum can be found using a set of atomic correlation functions. For $N = 2$ we obtain:

$$\langle a_k^\dagger(t)a_k(t) \rangle = \langle a_k^\dagger(t)a_k(t) \rangle_+ + \langle a_k^\dagger(t)a_k(t) \rangle_-, \quad (62a)$$

$$\langle a_k^\dagger(t)a_k(t) \rangle_+ = |gk|^2 \int_0^t d\tau \int_0^\tau d\tau' e^{-i\omega(\tau-\tau')} \Theta_k(\tau, \tau'), \quad (62b)$$

$$\langle a_k^\dagger(t)a_k(t) \rangle_- = |gk|^2 \int_0^t d\tau \int_\tau^t d\tau' e^{-i\omega(\tau-\tau')} \Theta_k(\tau, \tau'). \quad (62c)$$

where:

$$\begin{aligned} \Theta_k(\tau, \tau') &= \langle \sigma_+^{(1)}(\tau)\sigma_-^{(1)}(\tau') \rangle + \langle \sigma_+^{(2)}(\tau)\sigma_-^{(2)}(\tau') \rangle \\ &+ e^{-ikd} \langle \sigma_+^{(1)}(\tau)\sigma_-^{(2)}(\tau') \rangle + e^{ikd} \langle \sigma_+^{(2)}(\tau)\sigma_-^{(1)}(\tau') \rangle. \end{aligned} \quad (63)$$

In order to correctly calculate the two-time spin correlation functions we subdivide the whole spectrum (62a) into two parts, for positive time difference (62b) (when $\tau > \tau'$) and negative time difference (62c) (when $\tau < \tau'$).

We want to remind again that in (62) the positive $k = +\omega/v_g$ corresponds to a forward, right moving wave, while the negative $k = -\omega/v_g$ corresponds to a backward, left moving wave,

To find complete spectra (62a) one should calculate the two-time correlation functions using (43). From (47) we can express the lowering and raising spin operators in terms of basis set (46):

$$\sigma_+^{(1,2)} = \frac{1}{\sqrt{2}} (|S\rangle \langle G| \mp |A\rangle \langle G| + |E\rangle \langle S| \pm |E\rangle \langle A|), \quad (64a)$$

$$\sigma_-^{(1,2)} = \frac{1}{\sqrt{2}} (|G\rangle \langle S| \mp |G\rangle \langle A| + |S\rangle \langle E| \pm |A\rangle \langle E|), \quad (64b)$$

and by switching to a Heisenberg picture, we find:

$$\sigma_+^{(1,2)}(t) = \frac{1}{\sqrt{2}} (P_{SG}(t) \mp P_{AG}(t) + P_{ES}(t) \pm P_{EA}(t)), \quad (65a)$$

$$\sigma_-^{(1,2)}(t) = \frac{1}{\sqrt{2}} (P_{GS}(t) \mp P_{GA}(t) + P_{SE}(t) \pm P_{AE}(t)), \quad (65b)$$

Thus, one can find the complete spectra (62a) by calculating four two-time correlation functions with the already obtained transition operators (51) and (52).

For the positive time difference $\tau > \tau'$ we obtain the following general expression:

$$\begin{aligned} \langle a_k^\dagger(t)a_k(t) \rangle_+ &= |gk|^2 \int_0^t d\tau \int_0^\tau d\tau' e^{-i\omega(\tau-\tau')} \\ &\times [(1 + \cos(kd)) (\langle E| \langle P_{SG}(\tau - \tau') \rangle_0 |S\rangle \langle E| \langle P_{EE}(\tau') \rangle_0 |E\rangle + \langle E| \langle P_{ES}(\tau - \tau') \rangle_0 |S\rangle \langle E| \langle P_{EE}(\tau') \rangle_0 |E\rangle \\ &\quad + \langle S| \langle P_{SG}(\tau - \tau') \rangle_0 |G\rangle \langle E| \langle P_{SS}(\tau') \rangle_0 |E\rangle) \langle E| \rho_S(0) |E\rangle \\ &+ (1 - \cos(kd)) (\langle E| \langle P_{EA}(\tau - \tau') \rangle_0 |A\rangle \langle E| \langle P_{EE}(\tau') \rangle_0 |E\rangle - \langle E| \langle P_{AG}(\tau - \tau') \rangle_0 |A\rangle \langle E| \langle P_{EE}(\tau') \rangle_0 |E\rangle \\ &\quad + \langle A| \langle P_{AG}(\tau - \tau') \rangle_0 |G\rangle \langle E| \langle P_{AA}(\tau') \rangle_0 |E\rangle) \langle E| \rho_S(0) |E\rangle \\ &\quad + (1 + \cos(kd)) \langle S| \langle P_{SG}(\tau - \tau') \rangle_0 |G\rangle \langle S| \langle P_{SS}(\tau') \rangle_0 |S\rangle \langle S| \rho_S(0) |S\rangle \\ &\quad + (1 - \cos(kd)) \langle A| \langle P_{AG}(\tau - \tau') \rangle_0 |G\rangle \langle A| \langle P_{AA}(\tau') \rangle_0 |A\rangle \langle A| \rho_S(0) |A\rangle \\ &\quad + i \sin(kd) \langle A| \langle P_{AG}(\tau - \tau') \rangle_0 |G\rangle \langle A| \langle P_{AS}(\tau') \rangle_0 |S\rangle \langle S| \rho_S(0) |A\rangle \\ &\quad - i \sin(kd) \langle S| \langle P_{SG}(\tau - \tau') \rangle_0 |G\rangle \langle S| \langle P_{SA}(\tau') \rangle_0 |A\rangle \langle A| \rho_S(0) |S\rangle]; \end{aligned} \quad (66)$$

and for the negative time difference $\tau < \tau'$ we obtain:

$$\begin{aligned}
\left\langle a_k^\dagger(t) a_k(t) \right\rangle_- &= |g_k|^2 \int_0^t d\tau \int_\tau^t d\tau' e^{-i\omega(\tau-\tau')} \\
&\times [(1 + \cos(kd)) (\langle S | \langle P_{GS}(\tau' - \tau) \rangle_0 | E \rangle \langle E | \langle P_{EE}(\tau) \rangle_0 | E \rangle + \langle S | \langle P_{SE}(\tau' - \tau) \rangle_0 | E \rangle \langle E | \langle P_{EE}(\tau) \rangle_0 | E \rangle \\
&\quad + \langle G | \langle P_{GS}(\tau' - \tau) \rangle_0 | S \rangle \langle E | \langle P_{SS}(\tau) \rangle_0 | E \rangle) \langle E | \rho_S(0) | E \rangle \\
&+ (1 - \cos(kd)) (\langle A | \langle P_{AE}(\tau' - \tau) \rangle_0 | E \rangle \langle E | \langle P_{EE}(\tau) \rangle_0 | E \rangle - \langle A | \langle P_{GA}(\tau' - \tau) \rangle_0 | E \rangle \langle E | \langle P_{EE}(\tau) \rangle_0 | E \rangle \\
&\quad + \langle G | \langle P_{GA}(\tau' - \tau) \rangle_0 | A \rangle \langle E | \langle P_{AA}(\tau) \rangle_0 | E \rangle) \langle E | \rho_S(0) | E \rangle \\
&\quad + (1 + \cos(kd)) \langle G | \langle P_{GS}(\tau' - \tau) \rangle_0 | S \rangle \langle S | \langle P_{SS}(\tau) \rangle_0 | S \rangle \langle S | \rho_S(0) | S \rangle \\
&+ (1 - \cos(kd)) \langle G | \langle P_{GA}(\tau' - \tau) \rangle_0 | A \rangle \langle A | \langle P_{AA}(\tau) \rangle_0 | A \rangle \langle A | \rho_S(0) | A \rangle \\
&\quad - i \sin(kd) \langle G | \langle P_{GA}(\tau' - \tau) \rangle_0 | A \rangle \langle S | \langle P_{SA}(\tau) \rangle_0 | A \rangle \langle A | \rho_S(0) | S \rangle \\
&\quad + i \sin(kd) \langle G | \langle P_{GS}(\tau' - \tau) \rangle_0 | S \rangle \langle A | \langle P_{AS}(\tau) \rangle_0 | S \rangle \langle S | \rho_S(0) | A \rangle] \quad (67)
\end{aligned}$$

As is seen from (66), (67) only the initial density matrix of the form $\rho_S(0) = a|E\rangle\langle E| + b|A\rangle\langle A| + c|S\rangle\langle S| + d|A\rangle\langle S| + f|S\rangle\langle A|$, where a, b, c, d, f are arbitrary complex values, contributes to the radiation spectrum.

We can also calculate a total emission rate (37) for $N = 2$:

$$\begin{aligned}
W(t) &= \frac{\Gamma}{2} \left(\left\langle \sigma_+^{(1)}(t) \sigma_-^{(1)}(t) \right\rangle + \left\langle \sigma_+^{(2)}(t) \sigma_-^{(2)}(t) \right\rangle \right) \\
&+ e^{-ikd} \left\langle \sigma_+^{(1)}(t) \sigma_-^{(2)}(t) \right\rangle + e^{ikd} \left\langle \sigma_+^{(2)}(t) \sigma_-^{(1)}(t) \right\rangle \quad (68)
\end{aligned}$$

where $\langle \sigma_+^{(i)}(t) \sigma_-^{(j)}(t) \rangle$ can be found with $\tau = \tau' = t$ in either of equations (43). Thus, the emission rate can easily be calculated since it is proportional only to single-time correlation functions. With the help of expressions for spin operators (65) we can express (68) in terms of transition operators:

$$\begin{aligned}
W(t) &= \left(\Gamma \langle E | \langle P_{EE}(t) \rangle_0 | E \rangle + \frac{\Gamma_+}{2} \langle E | \langle P_{SS}(t) \rangle_0 | E \rangle \right. \\
&\quad \left. + \frac{\Gamma_-}{2} \langle E | \langle P_{AA}(t) \rangle_0 | E \rangle \right) \langle E | \rho_S(0) | E \rangle \\
&\quad + \frac{\Gamma_+}{2} \langle S | \langle P_{SS}(t) \rangle_0 | S \rangle \langle S | \rho_S(0) | S \rangle \\
&\quad + \frac{\Gamma_-}{2} \langle A | \langle P_{AA}(t) \rangle_0 | A \rangle \langle A | \rho_S(0) | A \rangle \\
&+ i \frac{\Gamma}{2} \sin(kd) \langle A | \langle P_{AS}(t) \rangle_0 | S \rangle \langle S | \rho_S(0) | A \rangle \\
&- i \frac{\Gamma}{2} \sin(kd) \langle S | \langle P_{SA}(t) \rangle_0 | A \rangle \langle A | \rho_S(0) | S \rangle \quad (69)
\end{aligned}$$

The expressions (66), (67), and (69) are the central result that we use in the following to calculate the super- and subradiant spectra and emission rates in two-qubit system for various initial configuration. They can be applied to any initial density matrix $\rho_S(0)$.

Below we consider several excited configurations of the two-qubit system. For every configuration we calculate the emission photon spectrum and the total rate of photon emission for different values of $k_0 d$. In order to make evident the influence of the second qubit on the radiation spectrum, we compare these quantities with those for a single qubit in the system.

In all figures to this section the radiation spectral densities and the emission rates are given in dimensionless units $S(\omega)2L\Omega/v_g$ and $W(t)/\Gamma$, respectively. All calculations are made for $\Gamma/\Omega = 0.05$.

A. Initial symmetric and asymmetric states

We start with initially prepared entangled states in the form of a symmetrical state $|\Psi(0)\rangle = (|e_1 g_2\rangle + |g_1 e_2\rangle)/\sqrt{2} = |S\rangle$ and an asymmetrical state $|\Psi(0)\rangle = (|g_1 e_2\rangle - |e_1 g_2\rangle)/\sqrt{2} = |A\rangle$. The experimental technique for the preparation of these entangled states is widely known in the circuit QED field and can be implemented by the sequence of Hadamard and CNOT gates [5].

As the qubit-photon coupling is efficient at $\omega \approx \Omega$, we perform subsequent calculations for $k \approx \pm k_0$ where $k_0 = \Omega/v_g$.

As is seen from (66), (67) the contribution of the symmetric and asymmetric initial states, $\rho_S(0) = |S\rangle\langle S|$, $\rho_S(0) = |A\rangle\langle A|$ are the even function of k . Therefore, the corresponding spectra are the same in both directions. From (66), (67), and (51b, 52f) we obtain:

$$\begin{aligned}
\left\langle a_k^\dagger(t) a_k(t) \right\rangle_S &= \\
&= \frac{v_g \Gamma_+}{2L} \frac{\left(e^{(i\delta_+ - \frac{\Gamma_+}{2})t} - 1 \right) \left(e^{-(i\delta_+ + \frac{\Gamma_+}{2})t} - 1 \right)}{\delta_+^2 + \frac{\Gamma_+^2}{4}}. \quad (70)
\end{aligned}$$

where we introduce the detuning parameters:

$$\delta_+ = \omega - \Omega_+; \quad \delta_- = \omega - \Omega_-; \quad (71)$$

If now we let time tend to infinity, $t \rightarrow \infty$, we get a radiation spectrum that is dependent only on the frequency:

$$S_S(\omega) = \frac{v_g}{2L} \frac{\Gamma_+}{(\delta_+^2 + \Gamma_+^2/4)} \quad (72)$$

For the total emission rate we obtain from (69) :

$$W_S(t) = \frac{\Gamma_+}{2} e^{-\Gamma_+ t} \quad (73)$$

The calculation procedure for asymmetric state $\rho_S(0) = |A\rangle\langle A|$ is very similar. For this initial state, we obtain for the spectrum, spectral density, and emission rate, respectively:

$$\langle a_k^\dagger(t) a_k(t) \rangle_A = \frac{v_g \Gamma_-}{2L} \frac{\left(e^{(i\delta_- - \frac{\Gamma_-}{2})t} - 1 \right) \left(e^{-(i\delta_- + \frac{\Gamma_-}{2})t} - 1 \right)}{\delta_-^2 + \frac{\Gamma_-^2}{4}} \quad (74)$$

$$S_A(\omega) = \frac{v_g}{2L} \frac{\Gamma_-}{(\delta_-^2 + \Gamma_-^2/4)} \quad (75)$$

$$W_A(t) = \frac{\Gamma_-}{2} e^{-\Gamma_- t} \quad (76)$$

Below we compare these quantities with those for an initially excited single qubit with the same frequency Ω and the decay rate Γ . For this case, the spectral density and the total emission rate are as follows:

$$S_1(\omega) = \frac{v_g}{2L} \frac{\Gamma}{(\omega - \Omega)^2 + \Gamma^2/4} \quad (77)$$

$$W_1(t) = \frac{\Gamma}{2} e^{-\Gamma t} \quad (78)$$

As is seen from (72) and (75) both spectra are Lorentzian lines whose central frequencies and the widths depend on $k_0 d$. The total emission rates (73) and (76) also depends on $k_0 d$. For Dicke case, $k_0 d = 0$, we obtain $W_A = 0$, $W_S = \Gamma e^{-2\Gamma t}$. The comparison of this result with (78) shows that the mere presence of a second unexcited qubit significantly alters the photon emission from excited qubit: its initial amplitude is twice as large as that for a single qubit and its decay proceeds at a twofold rate. This phenomenon is called a single photon super-radiance [15, 39] that can occur when a single-photon

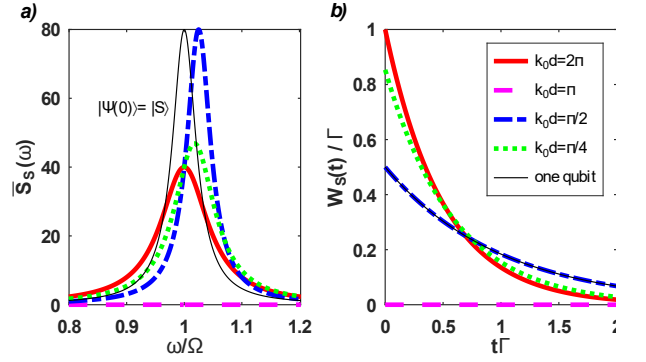


FIG. 1: a) Radiation spectra $\bar{S}_S(\omega) = S_S(\omega)2L\Omega/v_g$, expression (72), and b) Time dependence of the photon emission rate W_S/Γ , expression (73)), for initial symmetric state $|S\rangle$. For the comparison, the one-qubit case is shown by thin solid line; $\Gamma/\Omega = 0.05$.

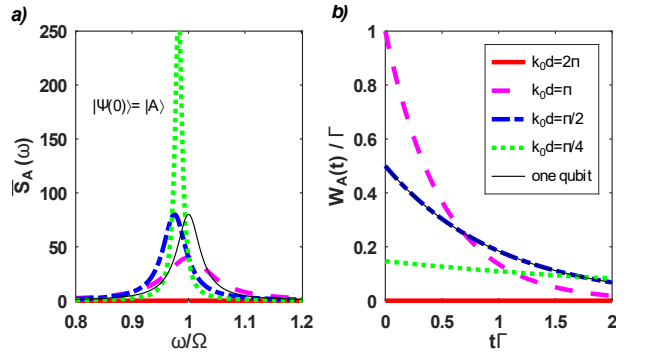


FIG. 2: a) Radiation spectra $\bar{S}_A(\omega) = S_A(\omega)2L\Omega/v_g$, expression (75), and b) Time dependence of the photon emission rate W_A/Γ , expression (76)), for initial asymmetric state $|A\rangle$. For the comparison, the one-qubit case is shown by thin solid line; $\Gamma/\Omega = 0.05$.

Dicke state is formed: N identical two level atoms are in a symmetrical superposition of states with one excited atom and $N - 1$ atoms in the ground state. In this case, the decay rate of a single photon is also equal to $N\Gamma$. The total radiated energy must be the same for both cases: $\int_0^\infty W_1(t)dt = \int_0^\infty W_S(t)dt$.

In relation to our problem it is important to note that contrary to free space in a one-dimensional geometry the Dicke case $k_0 d = 0$ occurs also for any $k_0 d = 2n\pi$, where n is positive integer.

The radiation spectra for initially states $|S\rangle$ and $|A\rangle$, together with the corresponding values of photon emission rates, W_S , W_A for different values of $k_0 d$ are shown in Fig. 1, Fig. 2, respectively.

From (73) we see that for $k_0 d = 2\pi$ a collective decay rate Γ_+ becomes equal to doubled decay rate of a single qubit: $\Gamma_+ = 2\Gamma$. This is shown by solid red line in Fig. 1b. The initial intensity of the photon emission is twice as large as that for a single qubit. The spectral line (solid red line in Fig. 1a) is not shifted. Its spectrum $S_S(\omega)$ is similar to the one for a single qubit, but with a dou-

bled line width and twofold decrease in the peak value. This is, in fact, is the manifestation of the Dicke superradiance, when the spectral line width is proportional to the number of atoms in the system, $N = 2$ in our case. For $k_0d = \pi/2$ the emission rates for two- and one-qubit systems are the same; dashed blue line in (Fig.1b) is superimposed on a single qubit line. Their spectral lines are identical but are shifted by $\Gamma/2$. If $k_0d = \pi$ the decay rate Γ_+ becomes zero, so that the symmetric state $|S\rangle$ does not radiate at all. Therefore, we may expect that in the vicinity of this value there exist a range of subradiant states with $\Gamma_{sub} \ll \Gamma$.

A different picture for the decay of initially asymmetric state $|A\rangle$ is shown in Fig.2. The superradiant emission is seen for $k_0d = \pi$ (purple dashed line in Fig.2b). For $k_0d = \pi/2$ the decay lines of emission rates for two- and single-qubit systems are superimposed (Fig.2b). The spectral line of a two-qubit system is identical to the one for a single qubit but is shifted to the left by $\Gamma/2$. A distinctive manifestation of the subradiant decay of asymmetric state is seen for $k_0d = \pi/4$ (green dashed line in Fig.2b). This decay is noticeably slower than the superradiant decay (purple dashed line in Fig.2b). The width of its spectral line is much smaller than that of a single qubit (purple dashed line in Fig.2a). If $k_0d = 2\pi$ the state $|A\rangle$ does not radiate. Here we also may expect the range of subradiant states with $\Gamma_{sub} \ll \Gamma$ in the vicinity of $k_0d = 2\pi$.

The only common feature of the decay of the states $|S\rangle$ and $|A\rangle$ is observed for $k_0d = (n + 1/2)\pi$ which corresponds to $\lambda_0 = 2d/(n + 1/2)$, where $\lambda_0 = 2\pi\Omega/v_g$. For this case, the radiating spectra for both symmetric and asymmetric states have the same linewidth $\Gamma_+ = \Gamma_- = \Gamma$, but their peaks are shifted in opposite directions because of the frequency shift $\delta_{\pm} = \omega - (\Omega \pm \Gamma/2)$. The evolution of their decay rates coincides with that for a single qubit.

We see from the Fig. 1, Fig. 2 that there are many subradiant states in the vicinity of $k_0d = \pi$ and $k_0d = 2\pi$ for initial $|S\rangle$ and $|A\rangle$ states, respectively. As the example, two subradiant states are shown in Fig. 3 for initial state $|S\rangle$. The widths of the emission spectra in Fig. 3a are equal to the corresponding decay rates in Fig. 3b.

B. Initial state with one excited qubit

Now we consider the initial state when only the first qubit is excited $|\Psi(0)\rangle = |e_1g_2\rangle$. The corresponding initial density matrix is given by:

$$\rho_S(0) = |eg\rangle \langle eg| = \frac{1}{2} |S - A\rangle \langle S - A| \quad (79)$$

From (79) it is seen, that two terms proportional to $|S\rangle \langle S|$ and $|A\rangle \langle A|$ provide the same result we calculated in the previous section. Hence, we only need to find the contribution of off-diagonal elements of $\rho(0)$.

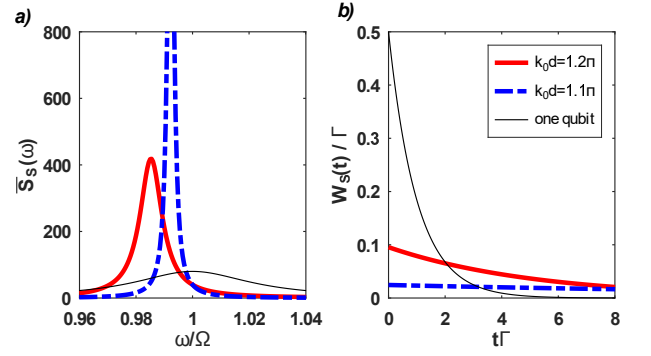


FIG. 3: Two subradiant decays of the initial $|S\rangle$ state for $k_0d = 1.2\pi$ (solid red line) and $k_0d = 1.1\pi$ (dashed blue line). (a) Radiation spectra $\overline{S}_S(\omega) = S_S(\omega)2L\Omega/v_g$; (b) Photon emission decay rate W_S/Γ . A single-qubit case is shown by thin solid line; $\Gamma/\Omega = 0.05$.

Using (66), (67), and explicit expressions for the transition operators (51a)-(51d), (52a)-(52f) we obtain the following expression:

$$\begin{aligned} \langle a_k^\dagger(t)a_k(t) \rangle_{eg} &= \frac{1}{2} \langle a_k^\dagger(t)a_k(t) \rangle_S + \frac{1}{2} \langle a_k^\dagger(t)a_k(t) \rangle_A \\ &+ i \frac{v_g\Gamma}{4L} \sin(kd) \left[\frac{(e^{-(i\delta_- + \Gamma_-/2)t} - 1)(e^{(i\delta_+ - \Gamma_+/2)t} - 1)}{(i\delta_- + \Gamma_-/2)(i\delta_+ - \Gamma_+/2)} \right. \\ &\quad \left. - \frac{(e^{-(i\delta_+ + \Gamma_+/2)t} - 1)(e^{(i\delta_- - \Gamma_-/2)t} - 1)}{(i\delta_+ + \Gamma_+/2)(i\delta_- - \Gamma_-/2)} \right] \quad (80) \end{aligned}$$

where the first two terms are given in (70) and (74). In the limit $t \rightarrow \infty$, we find frequency-dependent spectrum density:

$$\begin{aligned} S_{eg}(\omega) &= \frac{1}{2} S_S(\omega) + \frac{1}{2} S_A(\omega) \\ &- \frac{v_g\Gamma}{4L} \frac{\sin(kd)(\delta_- \Gamma_+ - \delta_+ \Gamma_-)}{(\delta_+^2 + \Gamma_+^2/4)(\delta_-^2 + \Gamma_-^2/4)} \quad (81) \end{aligned}$$

where $S_S(\omega)$ and $S_A(\omega)$ are given in (72) and (75). Finally, for the total emission rate we obtain:

$$\begin{aligned} W_{eg}(t) &= \frac{\Gamma_+}{4} e^{-\Gamma_+ t} + \frac{\Gamma_-}{4} e^{-\Gamma_- t} \\ &- \frac{\Gamma \sin(kd)}{2} e^{-\Gamma t} \sin(\Gamma \sin(k_0d) t) \quad (82) \end{aligned}$$

In the expressions (80), (81), and (82) first two terms correspond to the contribution from the states $|S\rangle$ and $|A\rangle$, while the second term results from the contribution of the off-diagonal matrix elements of the transition operator (last two lines in equations (66), (67), (69)). The backward and forward radiation corresponds to $k \approx -k_0$ and $k \approx +k_0$, respectively.

The forward radiation spectra and the forward emission decay rates are shown in Fig.4a and Fig.4b. Here, the interference terms in equations (81), and (82) significantly alter the picture. If k_0d is integer multiple

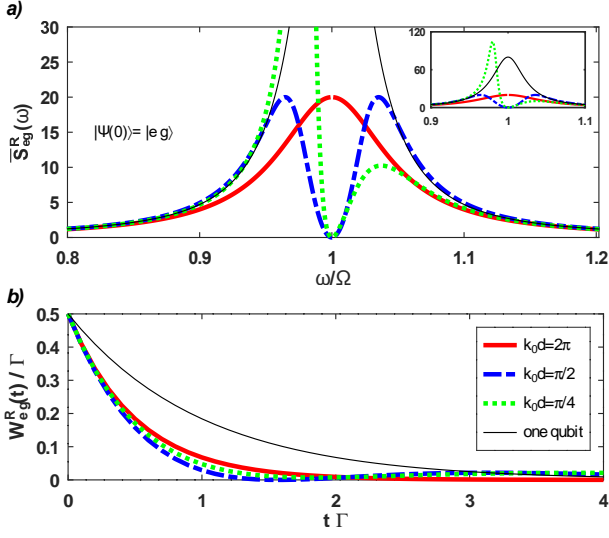


FIG. 4: a) The forward radiation spectra $\overline{S}_{eg}^L(\omega) = S_{eg}^L(\omega)2L\Omega/v_g$ for initially excited first qubit; b) The forward emission decay rate, W_{eg}^L/Γ for initially excited first qubit; For comparison a single-qubit case is shown by black thin line. $\Gamma/\Omega = 0.05$.

of π , then the interference term is zero. Therefore, for $k_0 d = 2\pi$ there is a superradiant state (red, solid line in Fig. 4a and b) with the decay rate being equal to 2Γ , $W_{eg}^L(t) = 0.5\Gamma e^{-2\Gamma t}$. In this case, the spectral line is a Lorentzian as shown in Fig. 4a. This effect which is known as single-atom [15] or single-photon [39] superradiance predicts the decay of excited atom at an enhanced rate in the presence of a second atom even though that second atom is in its ground state.

However, for other values of $k_0 d$ for which the interference term is not zero, the decay rate may also be as fast as the superradiance decay for $k_0 d = 2\pi$. For example, for $k_0 d = \pi/2$ we obtain from (82) $W_{eg}^L(t) = 0.5\Gamma e^{-\Gamma t}(1 - \sin(\Gamma t))$ (dashed blue line in Fig. 4b). Therefore, with respect to a single qubit case, all decay plots in Fig. 4b within the initial time scale, $0 < \Gamma t < 1$, may be considered as superradiant ones. In addition, the spectral line for $k_0 d = \pi/2$, dashed blue line in Fig. 4a, has a double peak symmetrical structure. A distance between the peaks is a measure of the coherent exchange interaction between qubits mediated by the continuum spectra of virtual photons. For this case, the inter-peak distance, which is determined by numerics, is 1.45Γ . By taking intermediate values of $k_0 d$ we can break this symmetry of interaction between the qubits. The plot of such asymmetric structure, which can be a signature of Fano resonance, is shown in Fig. 4a for $k_0 d = \pi/4$. It is also worth mentioning the absence of forward radiation at the qubit frequency for $k_0 d = \pi/2$ (dashed blue line in Fig. 4a). In this case, the radiation propagates from left to right, from the first, excited qubit, to the second, unexcited qubit, and does not penetrate behind the second qubit. The second qubit acts as an ideal mirror at

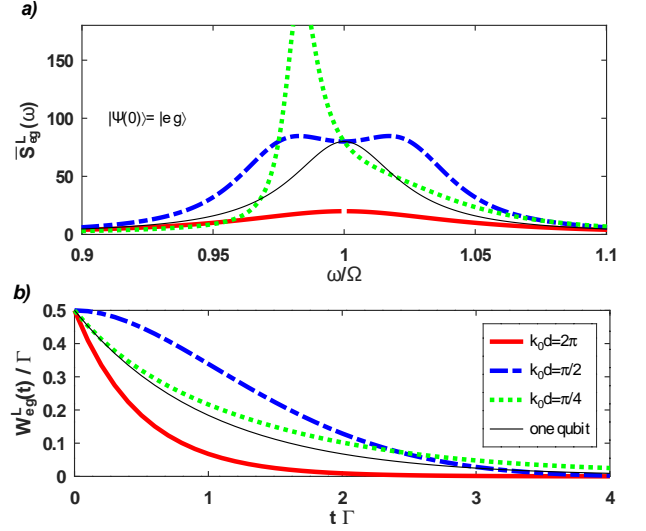


FIG. 5: a) The backward radiation spectra $\overline{S}_{eg}^R(\omega) = S_{eg}^R(\omega)2L\Omega/v_g$ for initially excited first qubit. b) The backward emission decay rate, W_{eg}^R/Γ for initially excited first qubit; For comparison a single-qubit case is shown by black thin line. $\Gamma/\Omega = 0.05$

this frequency. The same result was obtained in [32] by a different method.

The radiation spectra and the emission rate for backward scattering can be obtained from (81) and (82) for $k \approx -k_0$. The corresponding plots are shown in Fig. 5a, Fig. 5b. The inter-peak distance (dashed blue line in Fig. 5a, which is a measure of the photon mediated coupling between qubits, is approximately 0.68Γ . Here, a superradiant decay also takes place for $k_0 d = 2\pi$, where the interference terms in (81) and (82) are equal to zero. In this case, backward radiation is the same as that in the forward direction. However, for other values of $k_0 d$ for which the interference terms are not zero, the backward radiation is significantly different from the forward radiation which is seen by the comparison between Fig. 4a, Fig. 4b, and Fig. 5a, Fig. 5b.

If a second qubit is initially excited, $|\Psi(0)\rangle = |g_1 e_2\rangle$, then the density matrix becomes $\rho_S(0) = \frac{1}{2}|S+A\rangle\langle S+A|$. In this case, the result is given by the equations (80), (81), and (82) with the sign of last terms in these equations being changed. Therefore, for initially excited second qubit the equations (80), (81), and (82) (as they are written) describe the backward scattering for $k = +k_0$ and the forward scattering for $k = -k_0$.

Therefore, from (81) we may conclude that, in general, the probability to detect a photon by left or right detector is not equal to each other since the backward and forward radiation spectra are different. However, their sum, $S_S(\omega) + S_A(\omega)$ is not direction sensitive since it does not depend on the interference term. The emission rate (82), that is, the rate of the energy loss, is also different for backward and forward emission, however their sum, that is, the total emission rate, $W_S(t) + W_A(t)$ is

not direction sensitive.

C. Initial state with two excited qubits

Here we consider the spectrum for the initial state with both qubits being excited, $|\Psi(0)\rangle = |e_1e_2\rangle = |E\rangle$. The corresponding density matrix is $\rho_S(0) = |E\rangle\langle E|$. From (66), (67) we obtain the following result for the radiation spectrum:

$$\begin{aligned}
\left\langle a_k^\dagger(t)a_k(t) \right\rangle_E &= \frac{\Gamma_+}{\Gamma_-} \left\langle a_k^\dagger(t)a_k(t) \right\rangle_S + \frac{\Gamma_-}{\Gamma_+} \left\langle a_k^\dagger(t)a_k(t) \right\rangle_A \\
&+ \frac{v_g}{2L} \frac{\Gamma_+^2 + \Gamma_-^2}{2\Gamma} (e^{-2\Gamma t} - 1) \left[\frac{e^{-ik_0d}}{\Gamma_+ (1 + i \sin(k_0d)) (i\delta_- - \Gamma_-/2)} - \frac{e^{-ik_0d}}{\Gamma_- (1 - i \sin(k_0d)) (i\delta_+ - \Gamma_+/2)} \right. \\
&\quad \left. + \frac{e^{ik_0d}}{\Gamma_- (1 + i \sin(k_0d)) (i\delta_+ - \Gamma_-/2 - \Gamma)} - \frac{e^{ik_0d}}{\Gamma_+ (1 - i \sin(k_0d)) (i\delta_- - \Gamma_+/2 - \Gamma)} \right] \\
&+ \frac{v_g}{2L} \frac{e^{ik_0d}}{\Gamma_+ (1 - i \sin(k_0d))} \frac{(e^{-(i\delta_- + \Gamma_-/2)t} - 1) (\Gamma_-^2 + \Gamma_+^2 e^{(i\delta_- - \Gamma_+/2 - \Gamma)t})}{(i\delta_- + \Gamma_-/2) (i\delta_- - \Gamma_+/2 - \Gamma)} \\
&- \frac{v_g}{2L} \frac{e^{ik_0d}}{\Gamma_- (1 + i \sin(k_0d))} \frac{(e^{-(i\delta_+ + \Gamma_+/2)t} - 1) (\Gamma_+^2 + \Gamma_-^2 e^{(i\delta_+ - \Gamma_-/2 - \Gamma)t})}{(i\delta_+ + \Gamma_+/2) (i\delta_+ - \Gamma_-/2 - \Gamma)} \\
&+ \frac{v_g}{2L} \frac{e^{-ik_0d}}{\Gamma_- (1 - i \sin(k_0d))} \frac{(e^{-(i\delta_+ + \Gamma_-/2 + \Gamma)t} - 1) (\Gamma_-^2 + \Gamma_+^2 e^{(i\delta_+ - \Gamma_+/2)t})}{(i\delta_+ - \Gamma_+/2) (i\delta_+ + \Gamma_-/2 + \Gamma)} \\
&- \frac{v_g}{2L} \frac{e^{-ik_0d}}{\Gamma_+ (1 + i \sin(k_0d))} \frac{(e^{-(i\delta_- + \Gamma_+/2 + \Gamma)t} - 1) (\Gamma_+^2 + \Gamma_-^2 e^{(i\delta_- - \Gamma_-/2)t})}{(i\delta_- - \Gamma_-/2) (i\delta_- + \Gamma_+/2 + \Gamma)}
\end{aligned} \tag{83}$$

By taking time in (83) to infinity, we get the radiation spectral density:

$$\begin{aligned}
S_E(\omega) &= \frac{\Gamma_+}{\Gamma_-} S_S(\omega) + \frac{\Gamma_-}{\Gamma_+} S_A(\omega) + \frac{v_g}{2L} \frac{\Gamma_+^2 + \Gamma_-^2}{2\Gamma (1 + \sin^2(k_0d))} \left[\frac{e^{ik_0d} (1 + i \sin(k_0d))}{\Gamma_+ (i\delta_- - \Gamma_+/2 - \Gamma)} - \frac{e^{-ik_0d} (1 - i \sin(k_0d))}{\Gamma_+ (i\delta_- - \Gamma_-/2)} \right. \\
&\quad \left. + \frac{e^{-ik_0d} (1 + i \sin(k_0d))}{\Gamma_- (i\delta_+ - \Gamma_+/2)} - \frac{e^{ik_0d} (1 - i \sin(k_0d))}{\Gamma_- (i\delta_+ - \Gamma_-/2 - \Gamma)} \right] \\
&+ \frac{v_g}{2L} \frac{1}{(1 + \sin^2(k_0d))} \left[\frac{\Gamma_+^2}{\Gamma_+ (i\delta_- - \Gamma_-/2) (i\delta_- + \Gamma_+/2 + \Gamma)} \frac{e^{-ik_0d} (1 - i \sin(k_0d))}{(i\delta_- + \Gamma_-/2) (i\delta_- - \Gamma_+/2 - \Gamma)} - \frac{\Gamma_-^2}{\Gamma_+ (i\delta_- + \Gamma_-/2) (i\delta_- - \Gamma_+/2 - \Gamma)} \right] \\
&+ \frac{v_g}{2L} \frac{1}{(1 + \sin^2(k_0d))} \left[\frac{\Gamma_+^2}{\Gamma_- (i\delta_+ + \Gamma_+/2) (i\delta_+ - \Gamma_-/2 - \Gamma)} \frac{e^{ik_0d} (1 - i \sin(k_0d))}{(i\delta_+ - \Gamma_+/2) (i\delta_+ + \Gamma_-/2 + \Gamma)} - \frac{\Gamma_-^2}{\Gamma_- (i\delta_+ - \Gamma_+/2) (i\delta_+ + \Gamma_-/2 + \Gamma)} \right]
\end{aligned} \tag{84}$$

For the emission rate we obtain from (83):

$$W_E(t) = \frac{1}{2} \frac{\Gamma_+^2}{\Gamma_-} e^{-\Gamma_+ t} + \frac{1}{2} \frac{\Gamma_-^2}{\Gamma_+} e^{-\Gamma_- t} - \frac{4\Gamma \cos^2(k_0d)}{1 - \cos^2(k_0d)} e^{-2\Gamma t} \tag{85}$$

As might appear at the first sight the expressions (83-85) may take the infinite values for $k_0d = n\pi$ due to the widths Γ_-, Γ_+ in the denominator. However, a close inspection of these equations reveals that at these points the numerator is also zero. As previously, we can obtain the right solution if we put $k_0d = n\pi$ directly in the equations (49) and (50), or by expanding $\cos(k_0d)$ near $k_0d = n\pi$ in (83-85). For example, for $k_0d = 2\pi$ we find:

$$\begin{aligned}
\left\langle a_k^\dagger(t)a_k(t) \right\rangle_E \Big|_{k_0d=2\pi} &= 4 \frac{v_g \Gamma}{2L} \frac{(e^{-(i\delta+\Gamma)t} - 1) (e^{(i\delta-\Gamma)t} - 1)}{\delta^2 + \Gamma^2} + 2 \frac{v_g \Gamma}{2L} \frac{\Gamma^2}{i\delta (i\delta - \Gamma)^2 (i\delta - 2\Gamma)} \\
&+ 2 \frac{v_g \Gamma}{2L} \frac{e^{-2\Gamma t}}{(i\delta - \Gamma)^2} - 2 \frac{v_g \Gamma}{2L} \frac{e^{-(i\delta+2\Gamma)t} - 1}{i\delta (i\delta + 2\Gamma)} - 2 \frac{v_g \Gamma}{2L} \frac{e^{(i\delta-2\Gamma)t}}{i\delta (i\delta - 2\Gamma)} \\
&- 2 \frac{v_g \Gamma}{2L} \frac{2\Gamma}{(i\delta - \Gamma)^2} \frac{e^{-(i\delta+\Gamma)t} - 1}{(i\delta + \Gamma)} + 2 \frac{v_g \Gamma}{2L} \frac{2\Gamma}{(i\delta - \Gamma)} \frac{e^{(i\delta-\Gamma)t} - e^{-2\Gamma t}}{(i\delta + \Gamma)^2} + 2 \frac{v_g \Gamma}{2L} \frac{e^{-2\Gamma t}}{\delta^2 + \Gamma^2} 2\Gamma t
\end{aligned} \tag{86}$$

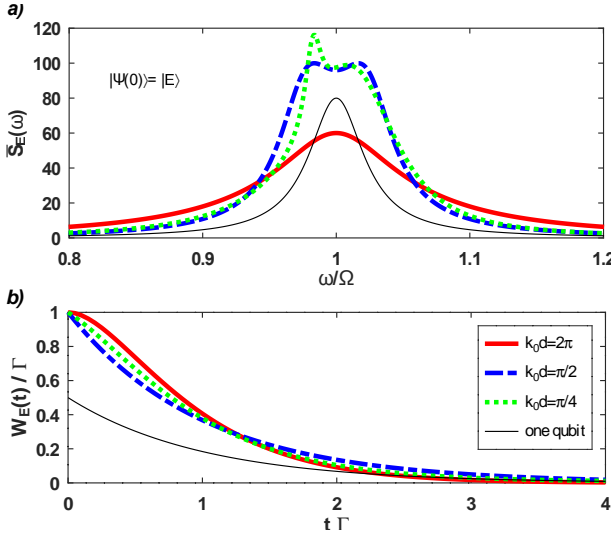


FIG. 6: a) Radiation spectra $\bar{S}_E(\omega) = S_E(\omega)2L\Omega/v_g$, expression (84), for two initially excited qubits (84) for different effective distances; b) Emission decay rate, $W_E(t)/\Gamma$ of two excited qubits (85); $\Gamma/\Omega = 0.05$.

$$S_E(\omega)|_{k_0 d=2\pi} = \frac{v_g}{2L} \frac{6\Gamma(\delta^2 + 2\Gamma^2)}{(\delta^2 + \Gamma^2)(\delta^2 + 4\Gamma^2)} \quad (87)$$

$$W_E(t)|_{k_0 d=2\pi} = (1 + 2\Gamma t) \Gamma e^{-2\Gamma t} \quad (88)$$

For this case, the radiation spectrum for several values of $k_0 d$ is shown in Fig.6a. For $k_0 d = n\pi$, where n is any integer, we obtain a single-peak Lorentzian line, though the analytical function (87) is more complex. For $k_0 d = \pi/2$ there are two peaks with a small separation at the top. Here, the inter-peak distance is approximately 0.66Γ . For $k_0 d = \pi/4$ there are two asymmetrical peaks which can be a signature of Fano resonance in the system.

The plots of emission decay rate for these values of $k_0 d$ are shown in Fig.6b. It is seen that the emission rates for two initially excited qubits are noticeably faster than the decay rate of a single qubit. Obviously, this is a signature of superradiant emission.

D. Initial states with qubits superposition

1. *First qubit is in a superposition state, a second qubit is in a ground state*

$$|\Psi(0)\rangle = |s_1\rangle \otimes |g_2\rangle = \frac{1}{\sqrt{2}}(|e_1\rangle + |g_1\rangle) \otimes |g_2\rangle = \frac{1}{2}|S\rangle - \frac{1}{2}|A\rangle + \frac{1}{\sqrt{2}}|G\rangle \quad (89)$$

The corresponding initial density matrix is given by:

$$\rho_S(0) = \frac{1}{4}(|S\rangle\langle S| + |A\rangle\langle A| - |S\rangle\langle A| - |A\rangle\langle S|) + \frac{1}{2\sqrt{2}}(|S\rangle\langle G| - |A\rangle\langle G| + |G\rangle\langle S| - |G\rangle\langle A|) + \frac{1}{2}|G\rangle\langle G| \quad (90)$$

The first line in (90) is a half of the density matrix of the state $|eg\rangle$ (79), therefore, we get the same spectrum and other related parameters similar to those for the first excited qubit (80-82), but reduced by the factor of two:

$$\langle a_k^\dagger(t)a_k(t) \rangle_{s_1 g_2} = \frac{1}{2} \langle a_k^\dagger(t)a_k(t) \rangle_{eg}; \quad (91)$$

$$S_{s_1 g_2}(\omega) = \frac{1}{2} S_{eg}(\omega); \quad W_{s_1 g_2}(t) = \frac{1}{2} W_{eg}(t);$$

The second line in (90) which describes the transitions to the ground state does not contribute to $\langle a_k^\dagger(t)a_k(t) \rangle$ (expressions (66), (67)).

Therefore the state with the first qubit prepared in a superposition state and the second one in a ground state shows the spectral properties identical to those shown in Figs. 4, 5, but on a smaller scale.

2. *First qubit is in a superposition state, a second qubit is in an excited state*

$$|\Psi(0)\rangle = |s_1\rangle \otimes |e_2\rangle = \frac{1}{\sqrt{2}}(|e_1\rangle + |g_1\rangle) \otimes |e_2\rangle = \frac{1}{\sqrt{2}}|E\rangle + \frac{1}{2}|S\rangle + \frac{1}{2}|A\rangle \quad (92)$$

and the corresponding initial density matrix is:

$$\rho_S(0) = \frac{|E\rangle\langle E|}{2} + \frac{|S\rangle\langle S| + |A\rangle\langle A| + |S\rangle\langle A| + |A\rangle\langle S|}{4} + \frac{|E\rangle\langle S| + |E\rangle\langle A| + |S\rangle\langle E| + |A\rangle\langle E|}{2\sqrt{2}} \quad (93)$$

As in the previous example, the first line in (93) corresponds to the initial states already considered above. Therefore, we can construct the spectrum and emission rate using (83) and ge counterpart of (80) (see the last paragraph in Sec.VIIB):

$$\langle a_k^\dagger(t)a_k(t) \rangle_{s_1 e_2} = \frac{1}{2} \langle a_k^\dagger a_k \rangle_E + \frac{1}{2} \langle a_k^\dagger a_k \rangle_{ge},$$

$$S_{s_1 e_2}(\omega) = \frac{1}{2} S_E(\omega) + \frac{1}{2} S_{ge}(\omega), \quad (94)$$

$$W_{s_1 e_2}(t) = \frac{1}{2} W_E(t) + \frac{1}{2} W_{ge}(t),$$

where $\langle a_k^\dagger a_k \rangle_{ge}$, $S_{ge}(\omega)$, and $W_{ge}(t)$ are given by the equations (80), (81), and (82) with the sign of the interference term in these equations being changed.

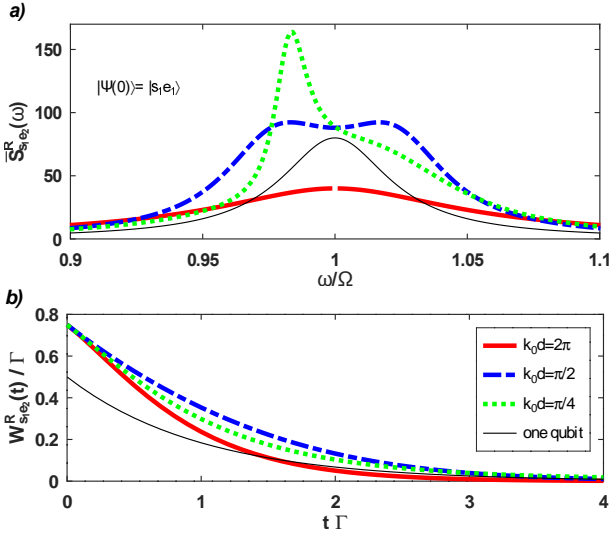


FIG. 7: a) Forward radiation spectra $\overline{S}_{s_1, e_2}^L(\omega) = S_{s_1, e_2}^L(\omega)2L\Omega/v_g$ for the initial state with the first qubit being in a superposition state and the second one being in the excited state for the different k_0d ; b) The forward emission decay rates $W_{s_1, e_2}^L/\Gamma$ for the same initial state; The single-qubit decay rate is $\Gamma/\Omega = 0.05$.

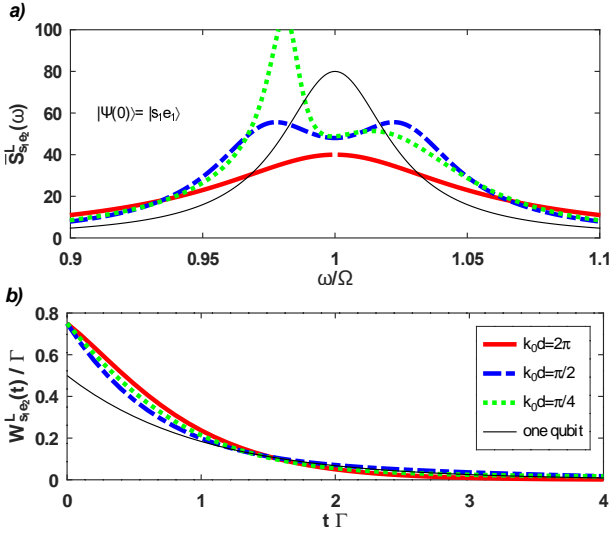


FIG. 8: a) Backward radiation spectra $\overline{S}_{s_1, e_2}^R(\omega) = S_{s_1, e_2}^R(\omega)2L\Omega/v_g$ for the initial state with the first qubit being in a superposition state and the second one being in the excited state for the different k_0d ; b) Backward emission decay rates $W_{s_1, e_2}^R/\Gamma$ for the same initial state; The single-qubit decay rate is $\Gamma/\Omega = 0.05$

Thus, the spectrum for the initial state (92) is a combination of the spectrum of two-excited qubits and that of a first excited qubit. Here, the probabilities for the photon to be emitted in left and right directions are different. The forward and backward radiation spectra and emission rates for this case are presented in Figs. 7a, 8a, and Figs. 7b, 8b, respectively.

3. Both qubits are initially prepared in a superposition state

$$\begin{aligned} |\Psi(0)\rangle &= \frac{1}{\sqrt{2}}(|e_1\rangle + |g_1\rangle) \otimes \frac{1}{\sqrt{2}}(|e_2\rangle + |g_2\rangle) \\ &= \frac{1}{2}|E\rangle + \frac{1}{\sqrt{2}}|S\rangle + \frac{1}{2}|G\rangle \end{aligned} \quad (95)$$

with the initial density matrix:

$$\begin{aligned} \rho_S(0) &= \frac{|E\rangle\langle E|}{4} + \frac{|S\rangle\langle S|}{2} \\ &\quad + \frac{|E\rangle\langle G| + |G\rangle\langle E| + |G\rangle\langle G|}{4} \\ &\quad + \frac{1}{2\sqrt{2}}(|E\rangle\langle S| + |S\rangle\langle E| + |S\rangle\langle G| + |G\rangle\langle S|) \end{aligned} \quad (96)$$

As it follows from (66), (67), only the first line in (96) contributes to the radiation spectrum, which can be presented as a combination of a two-excited qubit state (83-85) and a symmetrical state (70, 72, 73):

$$\begin{aligned} \langle a_k^\dagger(t)a_k(t) \rangle_{s_1s_2} &= \frac{1}{4}\langle a_k^\dagger a_k \rangle_E + \frac{1}{2}\langle a_k^\dagger a_k \rangle_S, \\ S_{s_1s_2}(\omega) &= \frac{1}{4}S_E(\omega) + \frac{1}{2}S_S(\omega), \\ W_{s_1s_2}(t) &= \frac{1}{4}W_E(t) + \frac{1}{2}W_S(t). \end{aligned} \quad (97)$$

For this case, the probabilities to find the photon in left or right detectors are the same. The characteristic plots for this case are presented in Figs. 9a, b. We see from Fig. 9b that the plot for $k_0d = \pi/2$ is superimposed on a single qubit plot. It means that the areas of corresponding spectral lines (Fig. 9a) are equal to each other, although their line shapes are different. Another feature is the existence of a subradiant state for $k_0d = \pi$, dashed purple line in Figs. 9a, 9b.

As a concluding remarks to this subsection we note that as can be seen from Fig. 7a, the radiation spectra for the initial state with the first qubit being in a superposition state and the other being in an excited state are very similar to the spectrum of two excited qubits shown in Fig. 6a. On the other hand, when both qubits are prepared in a superposition state, the spectrum changes significantly, and only for $k_0d = n\pi$ similarity is retained. Note that the line width of both spectrum (94) and (97) for $k_0d = 2\pi$ is identical. Moreover, it matches with the line width of the spectrum of two excited qubits (87) (red line in Fig. 6a).

VIII. CONCLUSION

In this paper we investigate superradiant and subradiant properties of the photon emission spectra for a two-qubit system coupled to one dimensional open waveguide. We obtain the general expression which allows

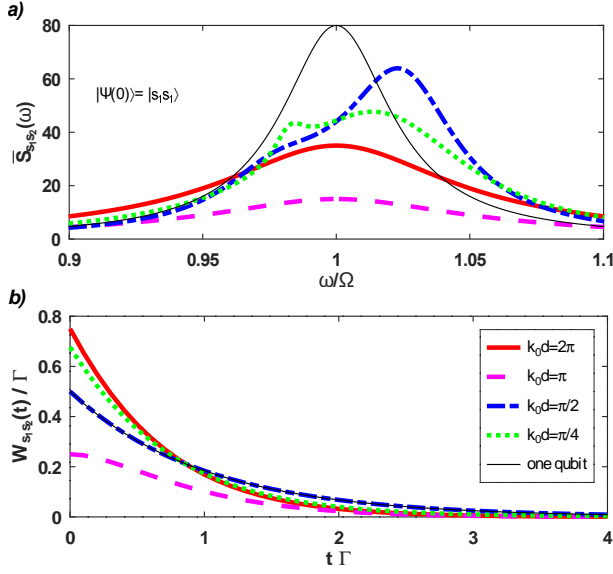


FIG. 9: a) Radiation spectra $\bar{S}_{s_1,s_2}(\omega) = S_{s_1,s_2}(\omega)2L\Omega/v_g$ for the state in which every qubit is initially in a superposition state; b) The emission decay rate $W_{s_1,s_2}/\Gamma$ for the initial superposition state; $\Gamma/\Omega = 0.05$.

us to calculate the radiation spectra for arbitrary initial configuration of a two-qubit system. We obtain the explicit expressions for the photon radiation spectra and the emission decay rates for different initial two-qubit configurations with one and two excitations. We show that the line shape of the photon radiation spectra and the emission decay rate, that is, the rate of the energy loss depend significantly on the effective distance between qubits, k_0d .

We believe that the results obtained in this paper may have practical applications in quantum information technologies including a control and optimization of the two-qubit entangling gates necessary for the realization of arbitrary unitary operations needed for quantum computation.

Acknowledgments

The work is supported by the Ministry of Science and Higher Education of Russian Federation under the project FSUN-2020-0004 and by the Foundation for the Advancement of Theoretical Physics and Mathematics "BASIS".

-
- [1] D. Roy, C. M. Wilson, and O. Firstenberg, Strongly interacting photons in one-dimensional continuum, *Rev. Mod. Phys.* **89**, 021001 (2017).
- [2] J. M. Raimond, M. Brune, and S. Haroche, Manipulating quantum entanglement with atoms and photons in a cavity, *Rev. Mod. Phys.* **73**, 565 (2001).
- [3] S. Noda, M. Fujita, and T. Asano, Spontaneous-emission control by photonic crystals and nanocavities, *Nat. Photon.* **1**, 449 (2007).
- [4] A. Blais, A. L. Grimsmo, S. M. Girvin, and A. Wallraff, Circuit quantum electrodynamics, *Rev. Mod. Phys.* **93**, 025005 (2021).
- [5] G. Wendin, Quantum information processing with superconducting circuits: a review, *Rep. Prog. Phys.* **80**, 106001 (2017).
- [6] X. Gu, A. F. Kockum, A. Miranowicz, Yu-xi Liu and F. Nori, Microwave photonics with superconducting quantum circuits, *Phys. Rep.* **718-719**, 1 (2017).
- [7] A. Wallraff, D. I. Schuster, A. Blais, L. Frunzio R-S. Huang, J. Majer, S. Kumar, S. M. Girvin and R. J. Schoelkopf, Strong coupling of a single photon to a superconducting qubit using circuit quantum electrodynamics, *Nature (London)* **431**, 162 (2004).
- [8] P. Forn-Diaz, L. Lamata, E. Rico, J. Kono and E. Solano, Ultrastrong coupling regimes of light-matter interaction, *Rev. Mod. Phys.* **91**, 025005 (2019).
- [9] R. H. Lehmborg, Radiation from an N-Atom system. I. General formalism, *Phys. Rev. A* **2**, 883 (1970).
- [10] R. H. Lehmborg, Radiation from an N-atom system. II. Spontaneous emission from a pair of atoms, *Phys. Rev. A* **2**, 889 (1970).
- [11] Z. Ficek and B. C. Sanders, Quantum beats in two-atom resonance fluorescence, *Phys. Rev. A* **41**, 359 (1990).
- [12] T. G. Rudolph, Z. Ficek, and B. J. Dalton, Two-atom resonance fluorescence in running- and standing-wave laser fields, *Phys. Rev. A* **52**, 636 (1995).
- [13] Z. Ficek and R. Tanas, Entangled states and collective non-classical effects in two-atom systems, *Phys. Repts.* **372**, 369 (2002).
- [14] G. Lenz and P. Meystre, Resonance fluorescence from two identical atoms in a standing-wave field, *Phys. Rev. A* **48**, 3365 (1993).
- [15] R. H. Dicke, Coherence in Spontaneous Radiation Processes, *Phys. Rev.* **93**, 99 (1954).
- [16] M. Gross and S. Haroche, Superradiance: an essay on the theory of collective spontaneous emission, *Phys. Rep.* **93**, 301 (1982).
- [17] K. Cong, Q. Zhang, Y. Wang, G. T. Noe II, A. Belyanin, and J. Kono, Dicke superradiance in solids, *J. Opt. Soc. Am. B* **33**, C80 (2016).
- [18] E. M. Purcell, Spontaneous Emission Probabilities at Radio Frequencies, *Phys. Rev.* **69**, 681 (1946).
- [19] A. Albrecht, L. Henriot, A. Asenjo-Garcia, P. B. Dieterle, O. Painter, and D. E. Chang, Subradiant states of quantum bits coupled to a one-dimensional waveguide, *New J. Phys.* **21**, 025003 (2019).
- [20] Y.-X. Zhang and K. Molmer, Theory of subradiant states of a one-dimensional two-level atom chain, *Phys. Rev. Lett.* **122**, 203605 (2019).
- [21] Ya. S. Greenberg, A. A. Shtygashev and A. G. Moiseev, Spontaneous decay of artificial atoms in a three-qubit system, *Eur. Phys. J. B* **94**, 221 (2021).
- [22] J. D. Brehm, A. N. Poddubny, A. Stehli, T. Wolz, H. Rotzinger, and A. V. Ustinov, Waveguide bandgap en-

- gineering with an array of superconducting qubits, npj Quantum Mater. **6**, 10 (2021).
- [23] M. Mirhosseini, E. Kim, Xu. Zhang, A. Sipahigil, P. B. Dieterle, A. J. Keller, A. Asenjo-Garcia, D. E. Chang, and O. Painter, Cavity quantum electrodynamics with atom-like mirrors, Nature (London) **569**, 692 (2019).
- [24] J. Q. You and F. Nori, Superconducting circuits and quantum information, Phys. Today **58**, 42 (2005).
- [25] S. N. Shevchenko, *Mesoscopic physics meets quantum engineering* (World Scientific, Singapore, 2019).
- [26] G. Ordóñez and S. Kim, Complex collective states in a one-dimensional two-atom system, Phys. Rev. A **70**, 032702 (2004).
- [27] K. Lalumière, B. C. Sanders, A. F. van Loo, A. Fedorov, A. Wallraff and A. Blais, Input-output theory for waveguide QED with an ensemble of inhomogeneous atoms, Phys. Rev. A **88**, 043806 (2013).
- [28] A. F. van Loo, A. Fedorov, K. Lalumière, B. C. Sanders, A. Blais, A. Wallraff, Photon-mediated interactions between distant artificial atoms, Science **342**, 1494 (2013).
- [29] M. Delanty, S. Rebec and J. Twamley, Superradiance and phase multistability in circuit quantum electrodynamics, New J. Phys. **13**, 053032 (2011).
- [30] N. Lambert, Y. Matsuzaki, K. Kakuyanagi, N. Ishida, S. Saito, and F. Nori, Superradiance with an ensemble of superconducting flux qubits, Phys. Rev. B **94**, 224510 (2016).
- [31] Fam Le Kien, S. D. Gupta, K. P. Nayak, and K. Hakuta, Nanofiber-mediated radiative transfer between two distant atom, Phys. Rev. A **72**, 063815 (2005).
- [32] A. A. Makarov and V. S. Letokhov, Spontaneous Decay in a System of Two Spatially Separated Atoms (One-Dimensional Case), J. Exper. and Theor. Phys. **97**, 688 (2003).
- [33] J. A. Mlynek, A. A. Abdumalikov, C. Eichler and A. Wallraff, Observation of Dicke superradiance for two artificial atoms in a cavity with high decay rate, Nat. Comm. **5**, 5186 (2014).
- [34] R. H. Lehmberg, Transition operators in radiative damping theory, Phys. Rev. **181**, 32 (1969).
- [35] A. Gonzalez-Tudela and D. Porras, Mesoscopic Entanglement Induced by Spontaneous Emission in Solid-State Quantum Optics, Phys. Rev. Lett. **110**, 080502 (2013).
- [36] C. M. Caves, Quantum limits on noise in linear amplifiers, Phys. Rev. D **26**, 1817 (1982).
- [37] C. Eichler, D. Bozyigit, A. Wallraff, Characterizing quantum microwave radiation and its entanglement with superconducting qubits using linear detectors, Phys. Rev. A **86**, 032106 (2012).
- [38] B. Kannan, D. L. Campbell, F. Vasconcelos, R. Winik, D. K. Kim, M. Kjaergaard, P. Krantz, A. Melville, B. M. Niedzielski, J. L. Yoder, T. P. Orlando, S. Gustavsson, W. D. Oliver, Generating spatially entangled itinerant photons with waveguide quantum electrodynamics, Sci. Adv. **6**, eabb8780 (2020).
- [39] M. O. Scully and A. A. Svidzinsky, The Super of Superradiance, Science **325**, 1510 (2009).